Adviesbureau ir. J.G. Hageman B.V.

Dossier 9032
QUAKESHIELD

Report 9032-1-4
Modelling of the out of plane behaviour

15nd of November 2017

Polakweg 14e
Postbus 26
2280 AA Rijswijk ZH

Telefoon 070 - 399 03 03
mail@adviesbureau-hageman.nl
www.adviesbureau-hageman.nl

CONTENT

1 Introduction 2

1.1 Order 2
1.2 Available data 2
1.3 Summary of available data 2
1.3.1 The system 2
1.3.2 Masonry properties 3
1.3.3 Pull out tests 4
1.3.4 Experimental research into out of plane behaviour 6
1.3.4.1 General 6
1.3.4.2 Static tests 6
1.3.4.3 Summary Moment-curvature relations 18

2 Analyses of results 18

2.1 Bond behaviour 18
2.2 Static out of plane behaviour 20
2.3 Structural behaviour of QSS+ specimens 21
2.4 Structural behaviour of QSS- specimens 24
2.5 Structural behaviour of QSP+ specimens 25
2.6 Structural behaviour of QSP- 28
2.7 Structural behaviour of QSC+ specimens 29
2.7.1 Introduction 29
2.7.2 First peak behaviour 30
2.7.3 Second peak behaviour 32
2.8 Structural behaviour of QSC- specimens 35
2.9 Adjustment of the model for the presence of axial loads and variable width 36
2.9.1 General 36
2.9.2 Capacity based on polymer strips 37
2.9.3 Capacity based on reinforced cement-matrix 39
2.10 Conclusion and summary 40

3 Determination of the design value of the resistance 41

4 Procedure to verify out of plane behaviour in seismic conditions 41

4.1 General 41
4.2 Example calculation A 42
4.3 Example calculation B 49
4.4 Example calculation C 52
4.4.1 General 52
4.4.2 Modelling different behaviour QSC wall 53
4.4.3 Checking QSC+ (stiff) 54
4.4.4 Checking QSC- (less stiff) 56

5 Summary 61

Annex A – NLTH Behaviour of Non-linear specimen

1 Introduction

1.1 Order

By QuakeShield B.V., a cooperation of Oosterhof Holman and SealteQ, a system is developed to enhance the structural properties of masonry walls. This system, named QuakeShield, improves the resistance of walls against seismic effects. To substantiate the use of the system, QuakeShield, in cooperation with the TU/e, performed experimental research that makes it possible to describe the structural behaviour of walls in which the system has been applied.

In this report, based on the experimental results, a model is described that can be used to determine the structural properties of masonry walls of which the properties are enhanced by applying QuakeShield.

In this third revision an additional model is described in which the capacity of the finishing of the cement based matrix under tension is considered.

1.2 Available data

The following data has been received from QuakeShield

1. Pull-out test of Carbon Fibre Reinforced Polymer (CFRP) strips installed in masonry wallettes with QuakeShield Epoxy, Vermeltfoort, A.T. and Ö.S. Türkmen;
2. Experiments to establish the moment-curvature correlation for QuakeShield reinforced clay brick masonry wallettes, Türkmen, Ö.S., 16th August 2016
3. Set of photo's of specimens described in [2]
4. Productbladen S&P ARMO-crete w(4) en S&P ARMO-mesh

1.3 Summary of available data

1.3.1 The system

QuakeShield consists of several components. It starts with the application of carbon fibre reinforced polymer strips (CFRP) in sleeves, placed in the middle of the masonry walls. The strips have a cross sectional dimension of 1,4×20 mm². The tension capacity of the strip is 78,4 kN. The Young's modulus equals 205 GPa. The connection between masonry and the CFRP-strips is provided by a visco-elastic adhesive QuakeShield Epoxy (Q-poxy).

Additional to this, a wall finishing can be applied on the side where the sleeves have been made. For this two types of finishing are available:

- a cement based matrix with an embedded CFRP-net
  the thickness of the cement-matrix is 15 à 20 mm
  the net is consisting of wires 3×0,044 mm² at a centre-to-centre distance of 20 mm in both directions
- a polymer based finishing
  the thickness of the layer is ± 5 mm

Material properties of these finishing's are described in table 2.3 of [2] which is summarized hereafter:

table 1 Properties of wall finishing

Property	unit	Cement layer with CFRP-net		Polymer
		Cement layer	CFRP-net	
density	kg/m³	2090	1790	1087
Young's modulus	GPa	26	160	1,2
tensile strength	MPa	6,5*	4300	45
compressive strength	MPa	45,5	-	38
max elongation	%	-	1,75	600

**) The results of the tests conducted on QuakeShield specimens show that 5,0 MPa is a more realistic value for the tensile strength. This value will be used in the calculations.*

In figure 1 the application of the system is shown. During the application first sleeves are created in the masonry wall. This can be done from the inside or the outside of the wall. The centre-to-centre distances between the sleeves can be varied. After this the CFRP-strips will be applied in a bed of Q-poxy. After this a finishing can be applied. In the figure the finishing consists of a CFRP-net over which a cement-matrix layer is applied.

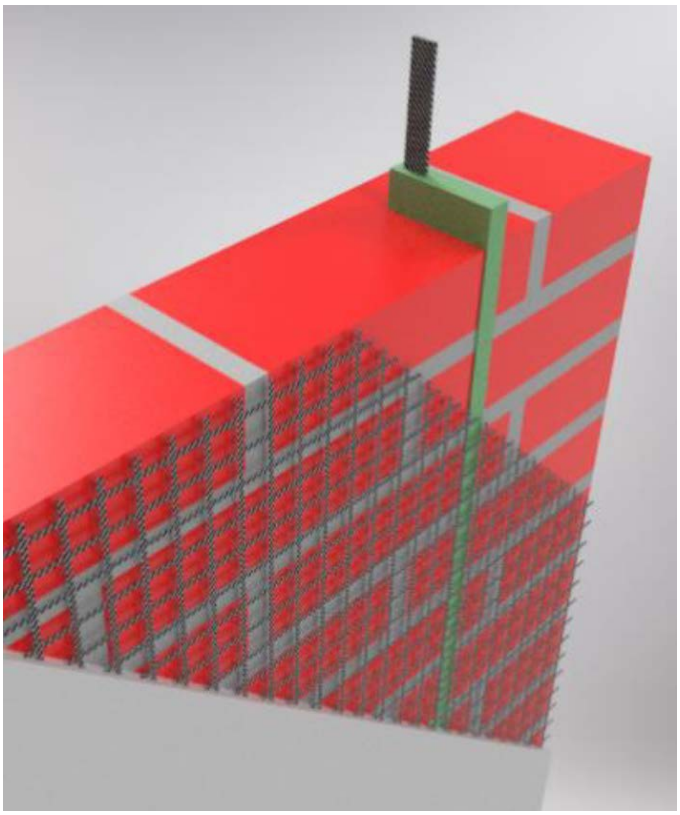

figure 1 Application of the QuakeShield system with a wall finishing of a cement based matrix with an embedded CFRP-net

1.3.2 Masonry properties

The masonry of the specimens was tested in separate tests. The masonry has the following properties:

mean compressive strength	f_{cm} = 7,08 N/mm²
mean flexure strength with a failure plane parallel to the bed joint	f_{xm} = 0,15 N/mm²

The applied mortar has the following properties:

mean compressive strength	6,42 N/mm²
mean flexure strength	2,51 N/mm²

1.3.3 Pull out tests

In [1] pull out tests on CFRP-strips connected with Q-poxy to masonry specimens are described. The tests are performed on CFRP-strips with different dimensions than the strips that are standard applied in the system. The properties of the strips used in the pull out tests and the standard strips are described in table 2.

table 2 Strip properties of pull out tests

Property	unit	CFRP-strip	
		pull out	standard
width	mm	15	20
thickness	mm	2,5	1,4
tensile capacity	kN	≥ 105	≥ 78,5
Young's modulus	GPa	≥ 170	≥ 205
elongation at break.	%	1,6	1,35

In the tests the CFRP-strips are embedded to the masonry over different lengths: 115, 175 and 230 mm. A picture of the specimens is shown in figure 2. For each length two tests have been performed.

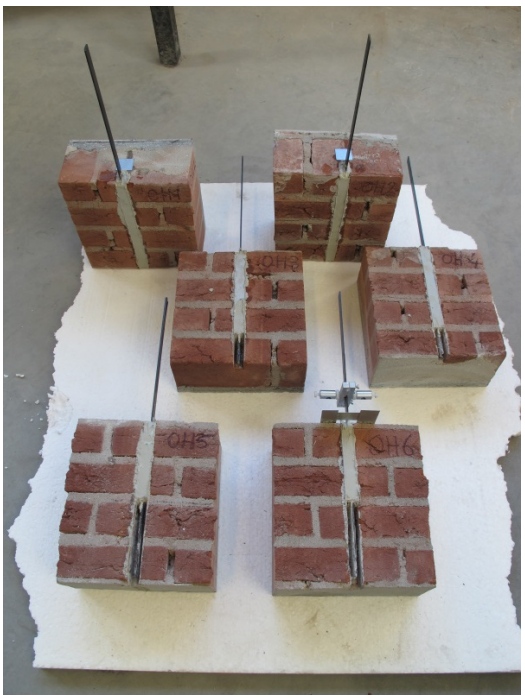

figure 2 Specimens for pull out tests

From the test results, summarized in figure 3, it shows that the ultimate pull out force is linear to the embedded length. It is described that the pull out force, expressed in kN, equals 50 times the embedded length in m.

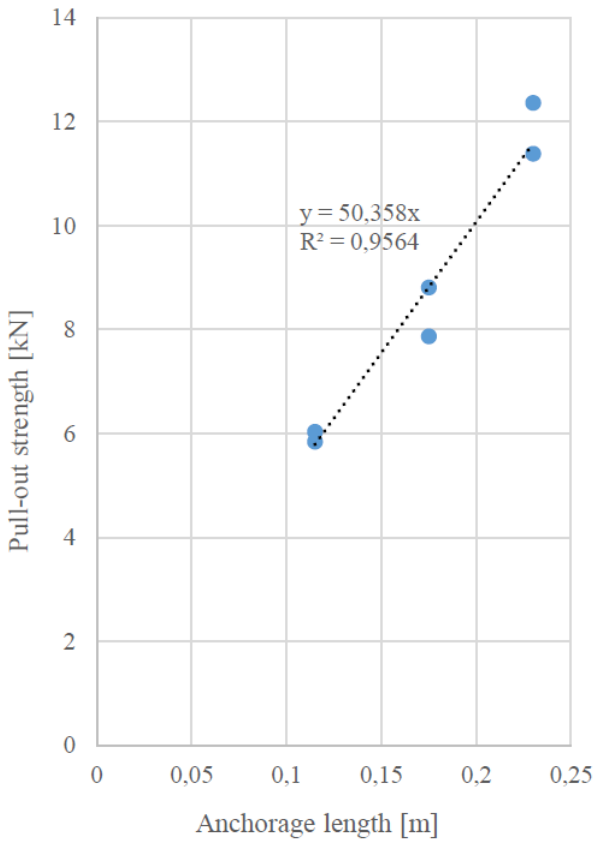

figure 3 Relation between embedded length and pull out force

During the tests the deformation difference between the CFRP-strip and the masonry, i.e. the bond-slip, at the side were the load is applied to the strip, was monitored. From this it shows that the force in the strip is increasing until the displacement difference equals 4 to 5 mm. After this the load in the strip is decreasing with an increase of displacement difference. The ultimate displacement differs for the several tests between 6,5 and 8,5 mm.

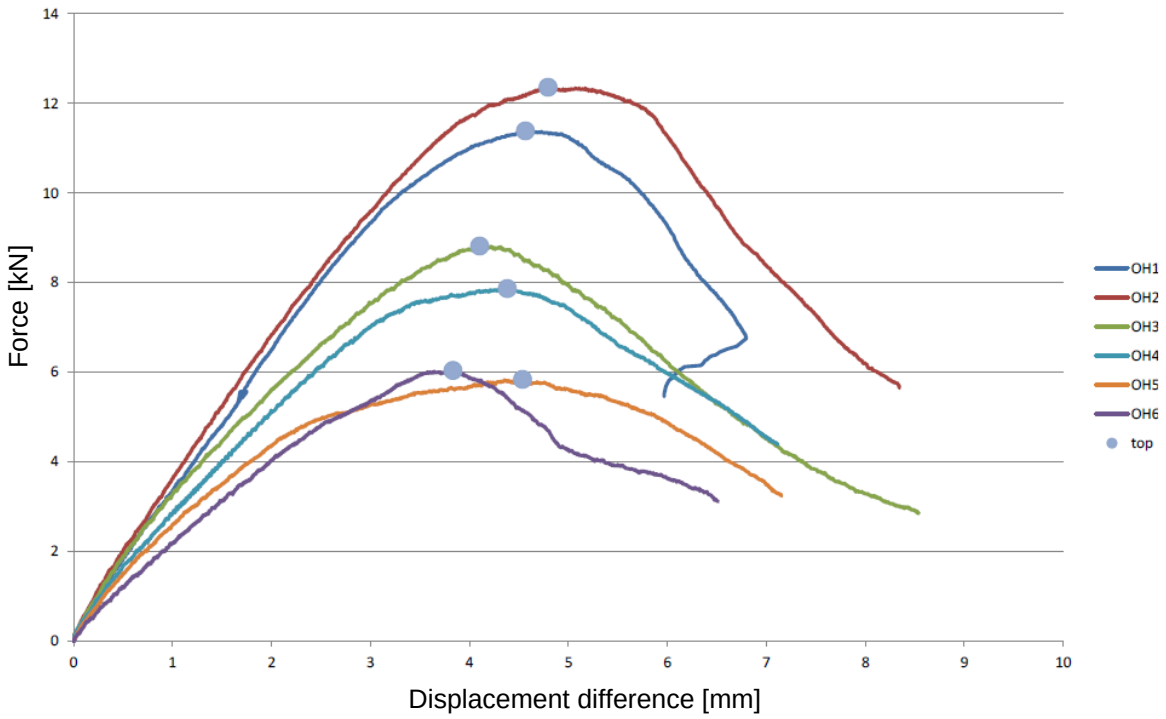

figure 4 Relation between displacement difference and pull out force for several embedded lengths

1.3.4 Experimental research into out of plane behaviour

1.3.4.1 General

In [2] an experimental research after the out of plane behaviour is described. The research consists of three types of tests:

- static four point bending tests from which the moment-curvature relation is determined;
- static cyclic three point bending test with axial loaded specimens and an increased out of plane deformation cyclic load;
- tests on the masonry.

In this report the dynamic three point bending test is not discussed.

1.3.4.2 Static tests

The static four point bending tests are applied to determine the moment-curvature relation and the resistance of masonry walls in which the QuakeShield system is applied. The research has been performed on clay brick masonry walls that have a width of 101 mm, a length of 650 mm and a height of 1250 mm. In all walls two CFRP-strips are applied.

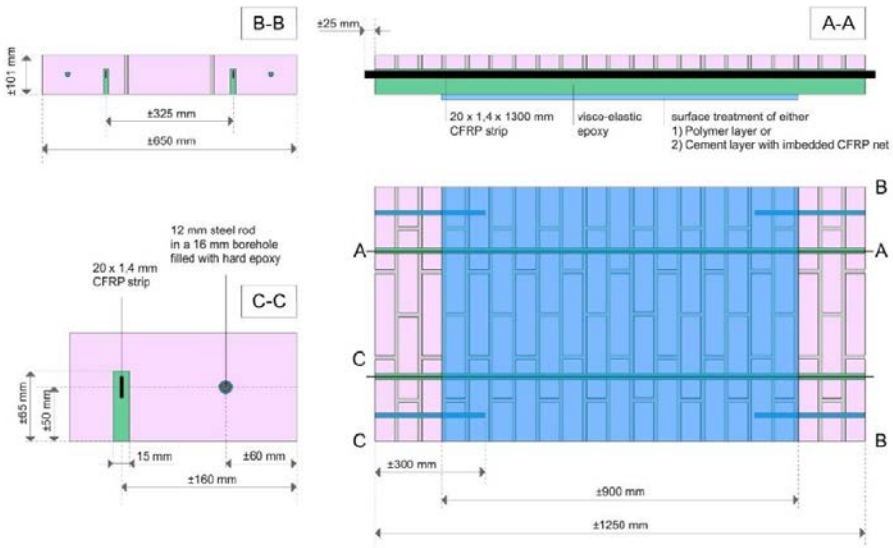

figure 5 Schematic overview of masonry specimens enhanced with QuakeShield

It should be noted that, as shown in figures 2.2 and 2.3 of [2], some of the specimens have, on one side of the masonry specimens, bed joints that are not filled until the face of the units. If this was the case, this side of the specimen has been used as the construction side where the sleeves and the finishing are applied.

Three configurations are created:

- QSS specimens in which only the two CFRP-strips are applied;
- QSP specimens with, beside the two CFRP-strips, a polymer based finishing;
- QSC specimens with, beside the two CFRP-strips, a finishing consisting of a CFRP-net and a cement-matrix.

The configurations are tested in two ways:
- with the construction side with the sleeves and eventually finishing on the tension side (+)
- with the construction side with the sleeves and eventually finishing on the compression side (-)

In total 5 configurations are tested, see table 3.

table 3 Tested configurations

	+	-
QSS	QSS+ 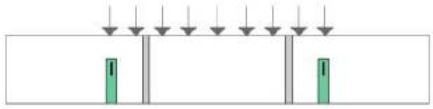	QSS- 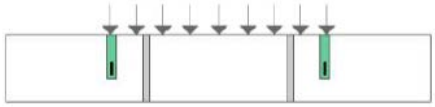
QSP	QSP+ 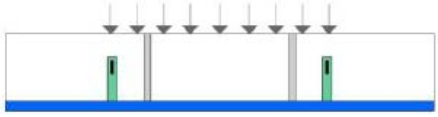	
QSC	QSC+	QSC- 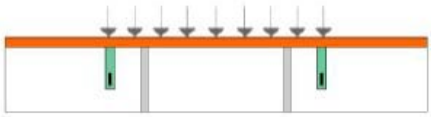

To improve the shear capacity, as is done in practice, at the end of the wall two steel rods are applied, see also figure 5.

The test set-up was a four point bending test, see figure 6. The finishing applied to the QSP and QSC specimens, is ended before the support of the specimen so to prevent for clamping the finishing between the masonry and the support which would enhance the anchorage of the finishing.

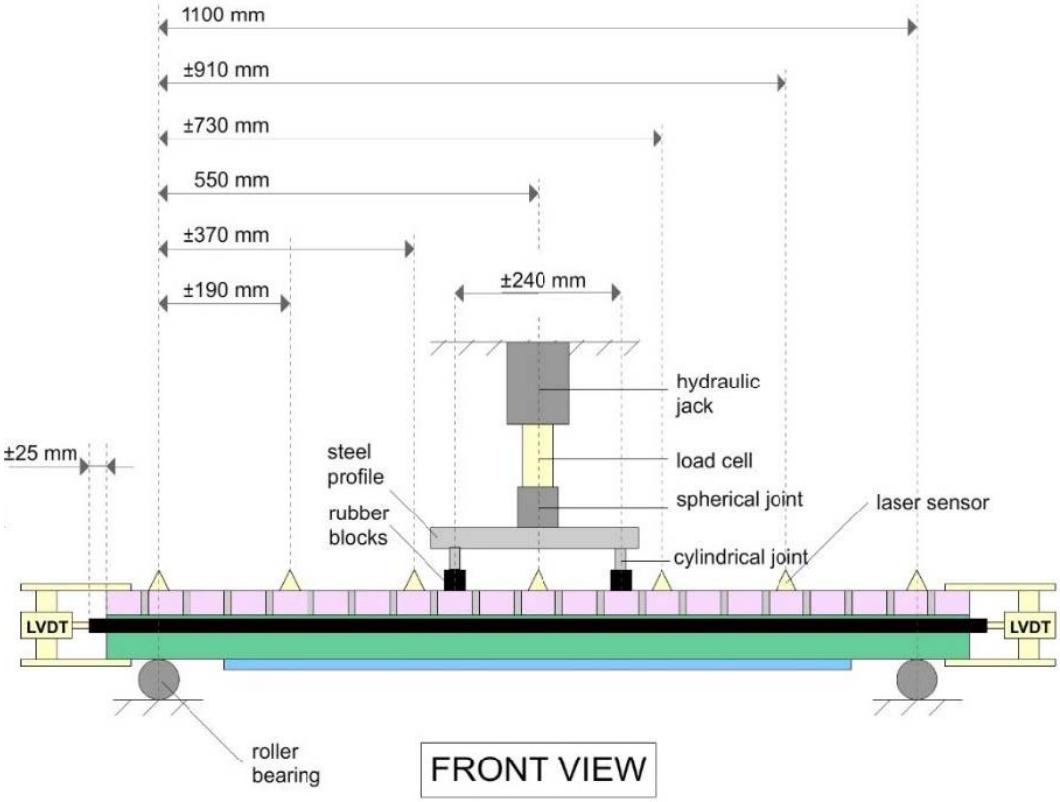

figure 6 Schematic overview of the four point bending test

During the test the out of plane displacement is measured. Beside that also the slip of the CFRP-strips at the end of the specimens is measured. The tests are continued until after reaching the maximum resistance, until the resistance has dropped to 90%. Unless otherwise stated the tests were finished because the maximum displacement of the jack was reached.

Hereafter the results of the performed tests are summarized.

QSS+

For this configuration 10 specimens have been tested. The mean value of the moment resistance is 2,46 kNm at a mean curvature of 0,55 m^{-1}. After the load decreased to 90% of the maximum the mean curvature increased to 0,63 m^{-1}. Both the load-displacement and the moment-curvature relations of the tests are shown in figure 7.

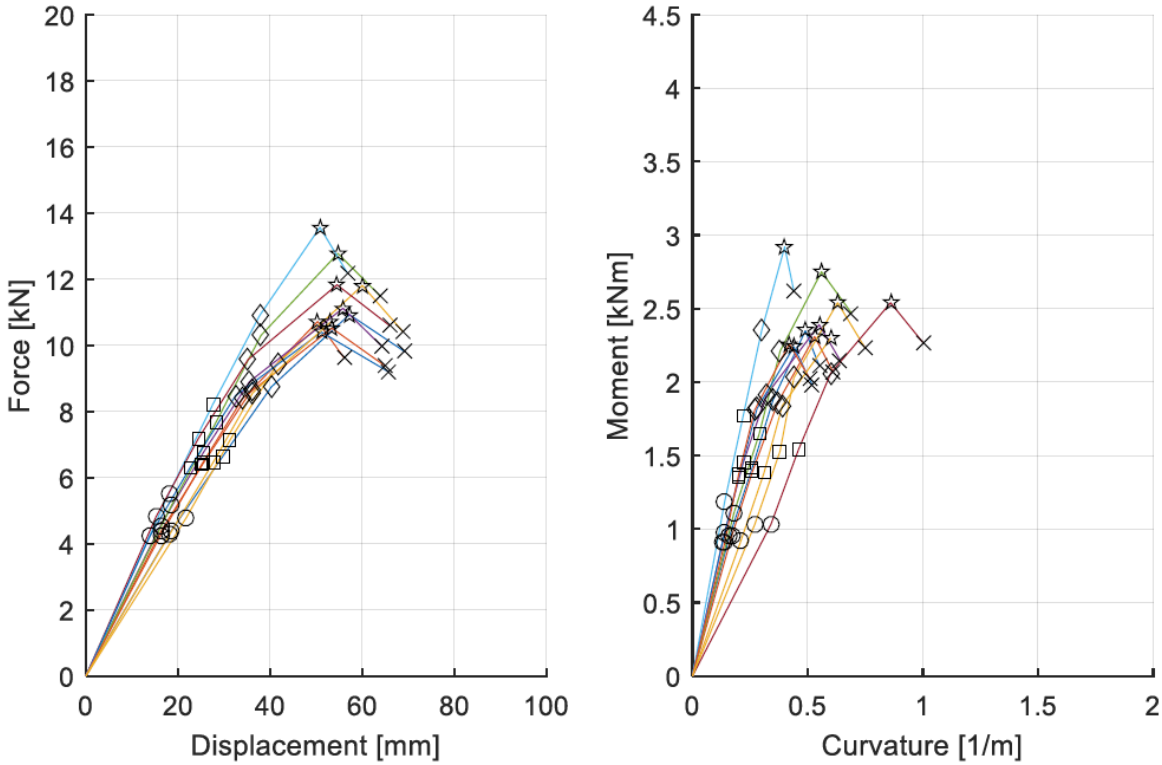

figure 7 Force-displacement and moment-curvature relations found for the QSS+ specimens

From the measurement of the slip of the CFRP-strips it can be concluded that the resistance of the specimens is determined by the bond capacity of the strips. When the maximum load is reached, the slip of the strips is increasing significantly. A typical behaviour of the slip is shown in figure 8. For both strips (1 and 2) slip starts to increase significantly at one of the supports when the maximum load is reached. At the other support the slip is decreasing with a decrease of the load and increase of the displacement.

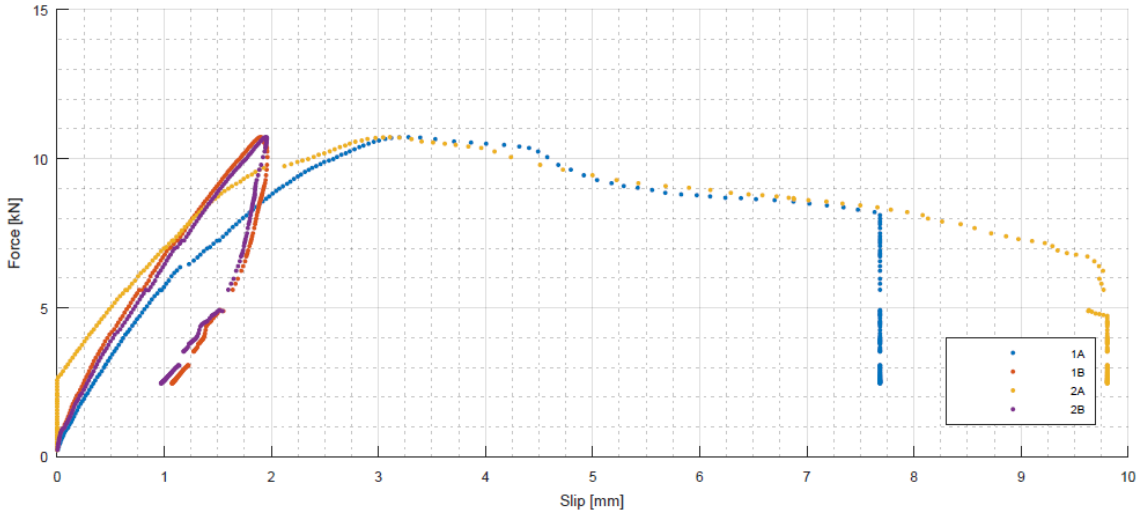

figure 8 Slip of CFRP-strips of specimen QSS+2

figure 9 Specimen QSS+6 at the end of the test

QSS-

For this configuration 11 specimens have been tested. The mean value of the moment resistance is 1,41 kNm at a mean curvature of 0,80 m^{-1}. After the load decreased to 90% of the maximum the mean curvature increased to 1,07 m^{-1}. Both the load-displacement and the moment-curvature relations of the tests are shown in figure 10.

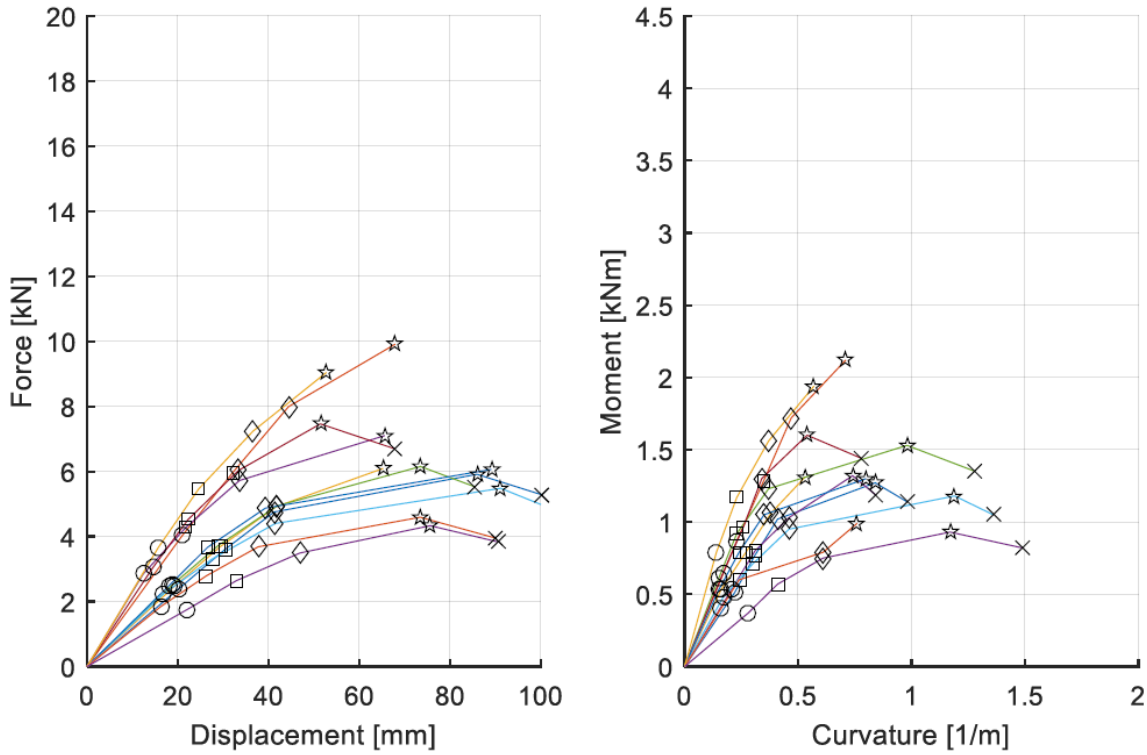

figure 10 Force-displacement and moment-curvature relations found for the QSS- specimens

The resistance of the QSS- specimens is lower than that of the QSS+ specimens. Also the variation of the results is much greater than is found for the QSS+ specimens. This difference is explained in [2]

Also for this configuration the slip of the CFRP-strips is increasing on one side of the strip from the moment the maximum resistance has been reached.

figure 11 Specimen QSS-1 at the end of the test

QSP+

For this configuration 11 specimens have been tested. The mean value of the moment resistance is 3,44 kNm at a mean curvature of 0,60 m^{-1}. After the load decreased to 90% of the maximum the mean curvature increased to 0,76 m^{-1}. Both the load-displacement and the moment-curvature relations of the tests are shown in figure 12.

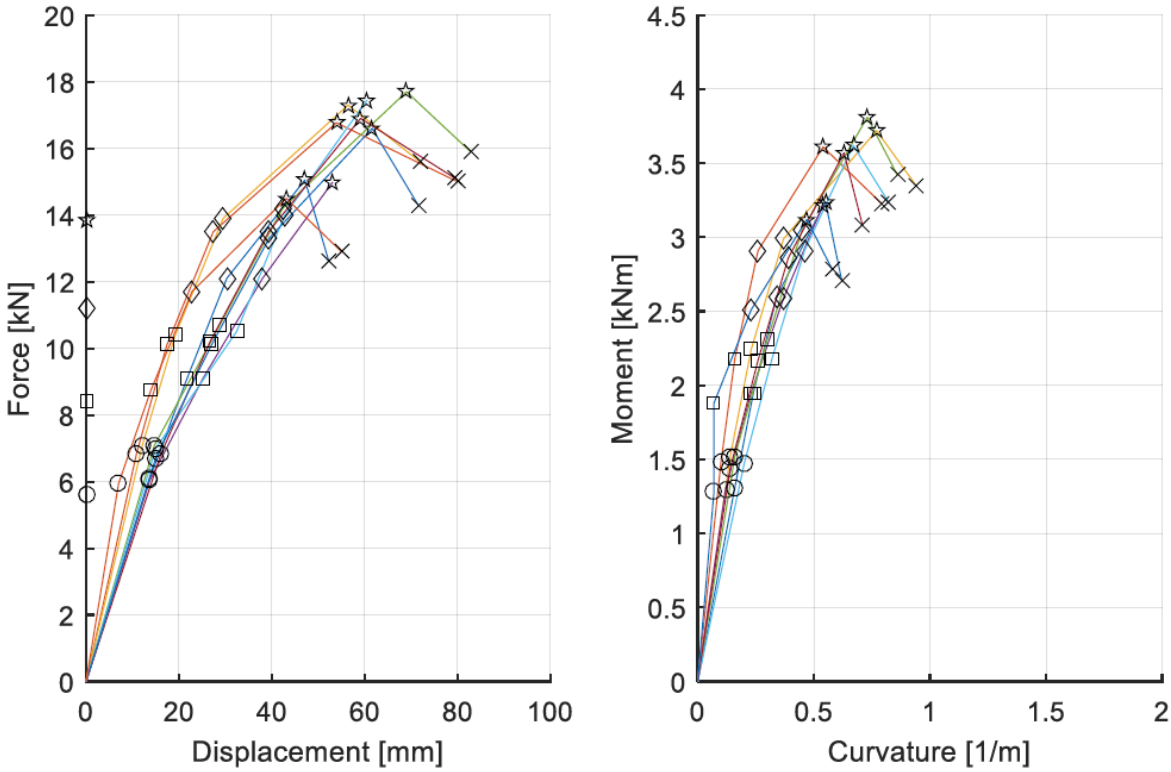

figure 12 Force-displacement and moment-curvature relations found for the QSP+ specimens

The resistance of the QSP+ specimens is greater than that of the QSS+ specimens. Except for QSP+9 an increase of the slip of the CFRP-strips is found when the maximum resistance is reached. A graph showing a typical relation between load and slip is shown in figure 13.

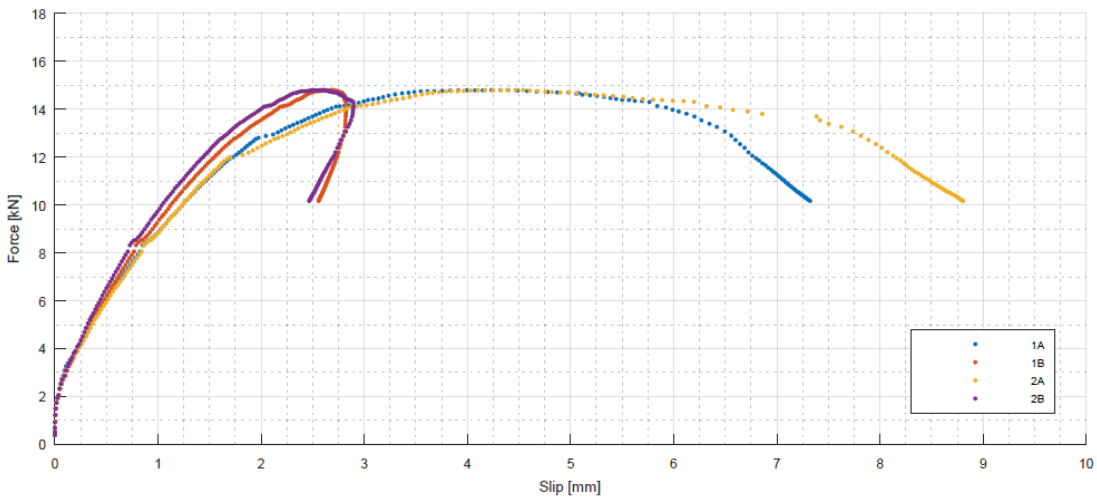

figure 13 Slip of CFRP-strips of specimen QSP+11

figure 14 Specimen QSP+2 at the end of the test

QSC+

The behaviour of the QSC+ specimens is quite different from the behaviour of the other configurations. First the test on the QSC+ specimens created some problems. At the first two tests, a brittle failure occurred due to cracks in the masonry just beside the end of the cement-matrix finish. This failure occurred before the first peak was reached. The failures occur while the maximum moment equals 2,88 and 3,16 kNm respectively. Values which are greater than the mean of the maximum resistance of the QSS+ specimens.

However to achieve a failure at midspan for the QSC+ specimens the test set-up was adjusted to a three point bending test. It should be noted that in the chosen set-up the finishing is clamped between the masonry wall and its supports, see figure 15.

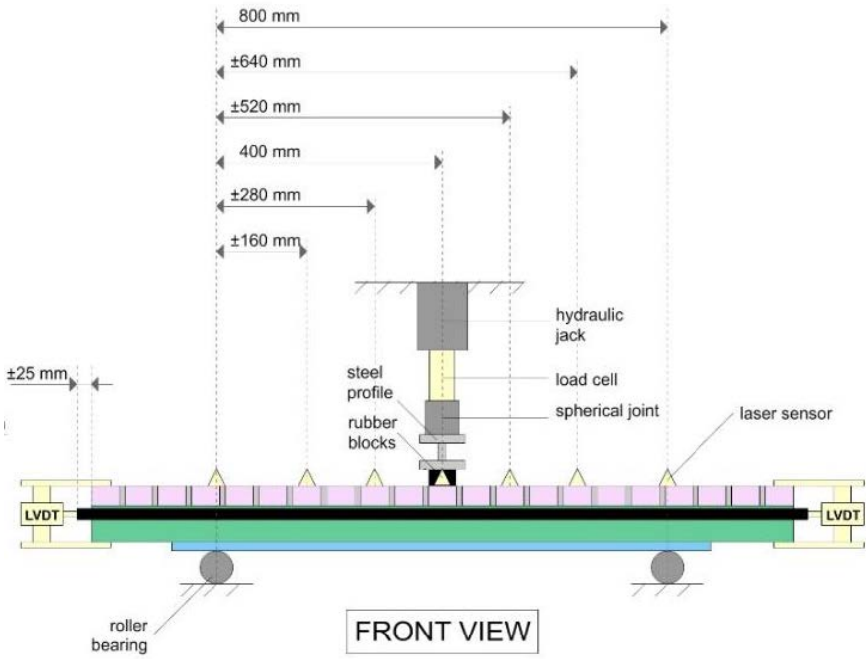

figure 15 Schematic overview of three point bending test for the QSC+ specimens

In the performed tests it is found that the QSC+ specimens have a higher capacity and a higher stiffness. However, after the maximum resistance is reached, the resistance of the specimen drops significantly and the specimens start to behave similar to the other configurations tested and reach a second peak for the resistance while the displacement is significant higher, see figure 16.

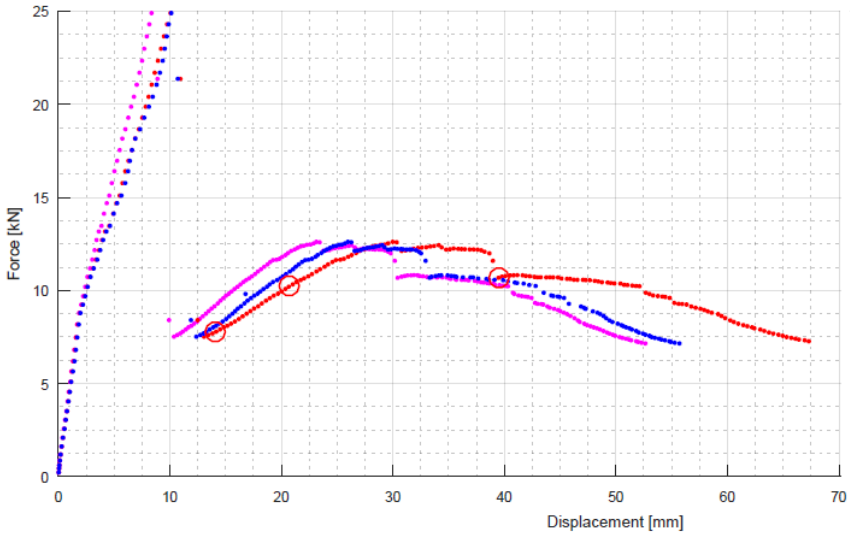

figure 16 External forces displacement relation for specimen QSC+1

For this configuration 10 specimens have been tested. Figure 17 shows the force-displacement relation of 6 of the specimens up until the first peak of the resistance. Because of wrong placement of the sensors, the other 4 specimens did not result in usable data. Therefore, these are not presented.

The mean values of the 6 specimens are shown with a black line. It consists of 2 linear parts, connecting the following values:

F1 = 12 kN δ1 = 2,5 mm

F2 = 24 kN δ2 = 7,5 mm

After reaching the peak force of approximately 24 kN, the force drops and displacements increase until a new, but smaller, peak force is reached. In figure 18 the force-displacement and moment-curvature relations for this second peak behaviour are presented.

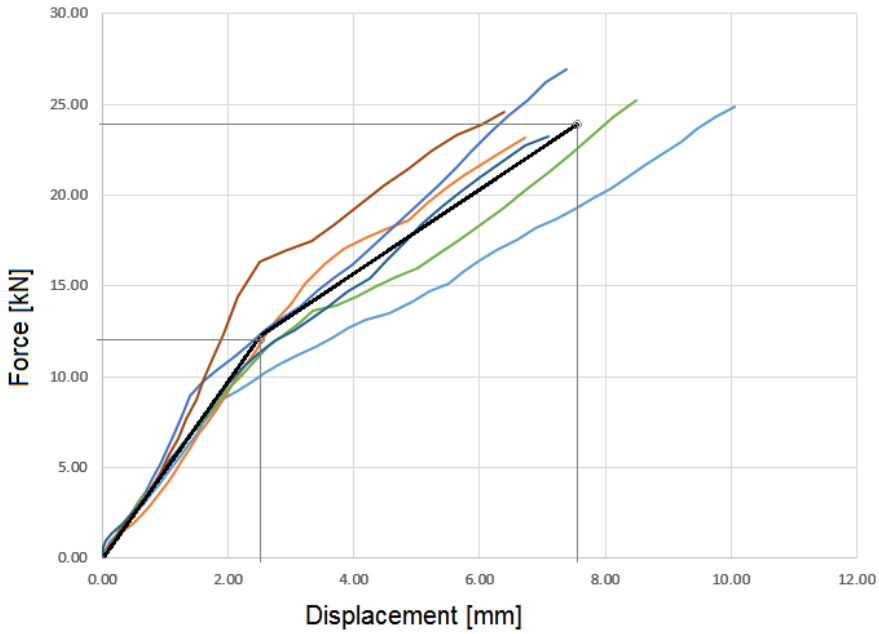

figure 17 Force-displacement relation found for the QSC+ specimens up until the first peak behaviour

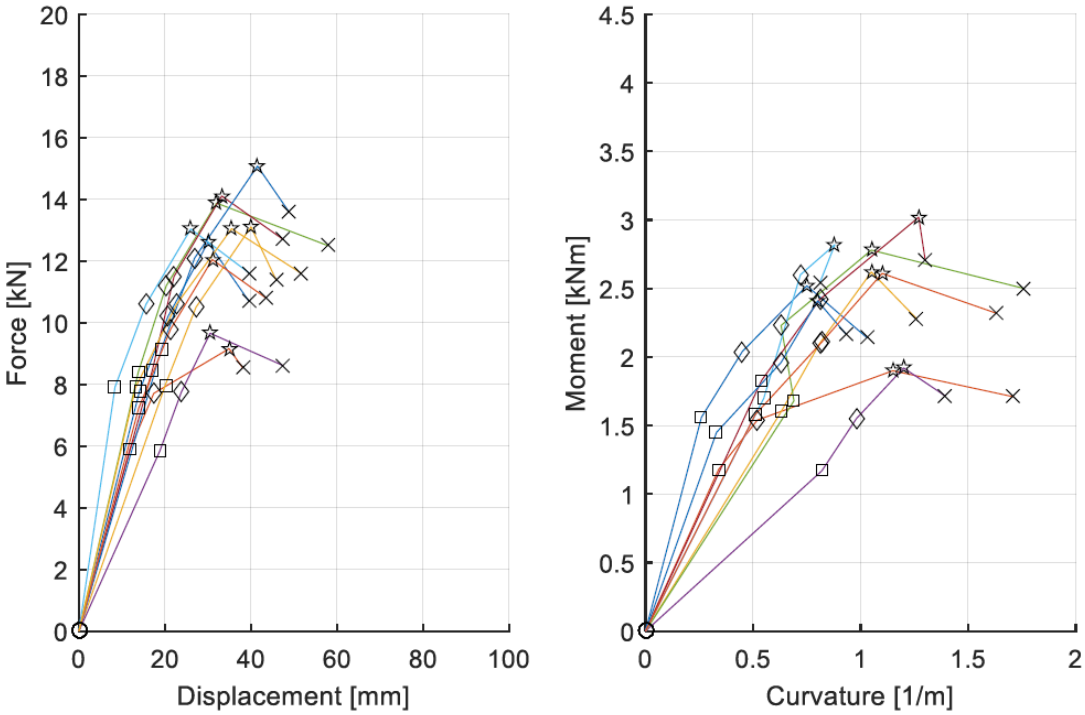

figure 18 Force-displacement and moment-curvature relations found for the QSC+ specimens without the registration of the first peak behaviour

The mean value of the moment resistance is 2,52 kNm at a mean curvature of 1,00 m^{-1}. After the load decreased to 90% of the maximum the mean curvature increased to 1,31 m^{-1}.

Identical to the other specimens for the QSC+ specimens the decrease of resistance occurs when the slip of the CFRP-strips increases.

figure 19 Specimen QSC+1 at the end of the test

QSC-

These specimens have been tested with the four point bending test as shown in figure 6.

For this configuration 11 specimens have been tested. The mean value of the moment resistance is 3,40 kNm at a mean curvature of 0,43 m^{-1}. After the load decreased to 90% of the maximum the mean curvature increased to 0,57 m^{-1}. Both the load-displacement and the moment-curvature relations of the tests are shown in figure 20.

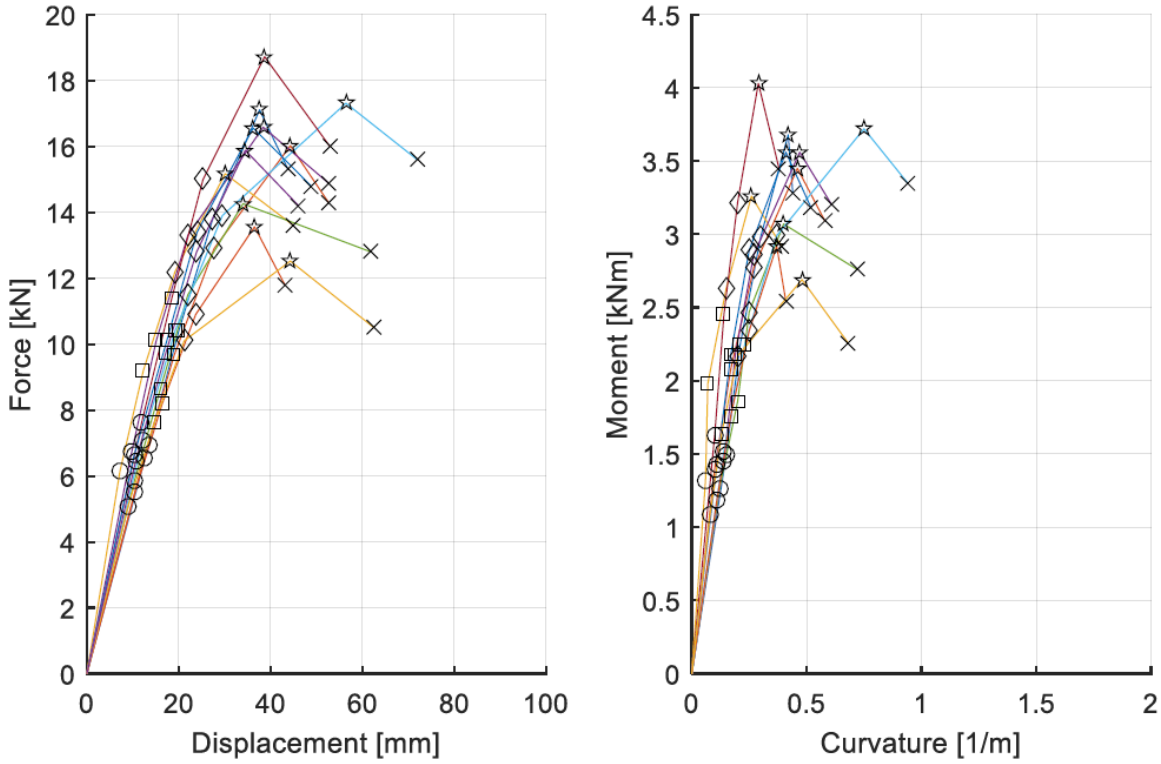

figure 20 Force-displacement and moment-curvature relations found for the QSC- specimens

The resistance of the QSC- specimens is greater than that of the QSS- specimens. Identical to the other specimens for the QSC- specimens the decrease of resistance occurs when the slip of the CFRP-strips increases.

figure 21 QSC-5 at the end of the test

1.3.4.3 Summary Moment-curvature relations

Based on the previous summarized results, hereafter the mean load-displacement and the mean moment-curvature relations, as determined by the experimental research, are presented for the considered configurations.

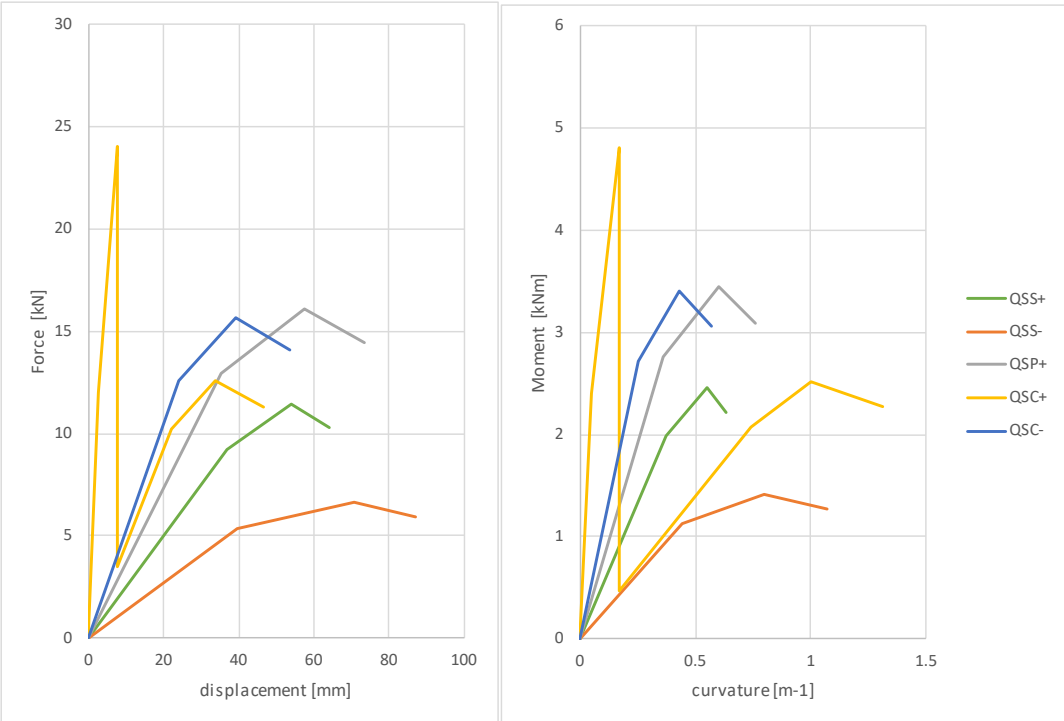

figure 22 Force-displacement and moment-curvature relations for the several configurations

Analysis of the results and the differences between the several configurations are discussed in section 3 of this report.

2 Analyses of results

2.1 Bond behaviour

From the pull out tests the bond behaviour of the CFRP-strip in the masonry, ensured by the Q-poxy, is derived.

From the material properties of the CFRP-strips, see table 2, the elongation of the strips under the ultimate pull out force can be calculated. In this calculation it is assumed that the force in the strip decreases linear over the embedded length. Hereafter the elongation is calculated for a strip with an embedded length of 175 mm and a maximum pull out force of 8,75 kN:

$$\Delta_s = \frac{F l_{em}}{2 E A} = \frac{8750 \cdot 175}{2 \cdot 170 \cdot 10^3 \cdot 15 \cdot 2{,}5} = 0{,}12 \text{ mm}$$

From a comparison of this value for Δ_s with the displacement difference that is described in paragraph 1.3.2, with a value of at least 4 mm, it shows that this displacement difference is significantly greater than the elongation of the strip. So it can be concluded that the bond behaviour of the CFRP-strip is determined by the properties of the Q-poxy only and that the distribution of the shear force between the strip and the masonry may be assumed to be uniform.

The maximum pull-out force can be derived from the embedded length l_{em}:
$F_s = K_Q\ l_{em}$

where:
$K_Q = 50$ N/mm

The relation between the displacement difference between the strip and the masonry and the force between these two can be described by the following equation:

$q_s = 15\ \Delta_s$	when $\Delta_s \leq 3$ mm
$q_s = 45 + 5(\Delta_s - 3)$	when 3 mm $< \Delta_s \leq 4$ mm
$q_s = 50 – 5{,}7(\Delta_s - 4)$	when 4 mm $< \Delta_s \leq 7$ mm
$q_s = 0$	when 7 mm $< \Delta_s$

with:
q_s is the shear force between strip and masonry per unit of length [N/mm]
Δ_s is the displacement difference between strip and masonry [mm]

The force in the strip F_s follows from:

$F_s = q_s\ l_{em}$

In figure 23 as a result of the relation of F_s with the displacement difference and the embedded length is given. This figure can be compared with figure 4. From this comparison it shows that the given relation between the shear force per unit of length and the displacement difference described the bond behaviour of the CFRP-strips quite well.

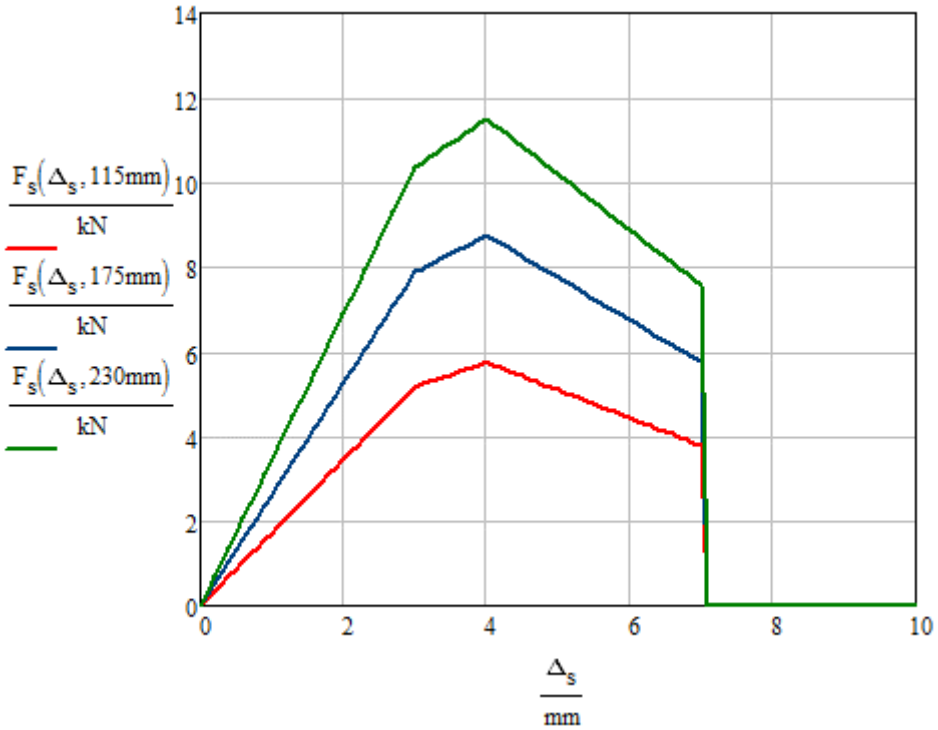

figure 23 Tension force in CFRP-strip as function of displacement difference Δl for several embedded lengths

It is concluded that the bond behaviour of the CFRP-strips can be described by:

$q_s = 15\ \Delta_s$	when $\Delta_s \leq 3$ mm
$q_s = 45 + 5(\Delta_s - 3)$	when 3 mm $< \Delta_s \leq 4$ mm
$q_s = 50 – 5{,}7(\Delta_s - 4)$	when 4 mm $< \Delta_s \leq 7$ mm
$q_s = 0$	when 7 mm $< \Delta_s$

where:
q_s is the shear force between strip and masonry per unit of length [N/mm]
Δ_s is the displacement difference between strip and masonry [mm]

Due to the lack of stiffness of the Q-poxy it can be concluded that the bond length may be taken from the point of maximum moment to the point of contraflexure or the end of the beam.

It should be noted that the CFRP-strips used in the experiments described in [1] are not identical to those used in the experiments described in [2]. In the absence of additional information it is assumed that the bond behaviour of the CFRP-strips in [2] is as described here.

2.2 Static out of plane behaviour

When the masonry walls would not have been strengthened with the QuakeShield system, the moment resistance of a cross section of the walls would have been limited to:

$M_{Rd} = f_{xm}\ W = 0{,}15 \cdot \frac{1}{6} 650 \cdot 101^2 = 165 \cdot 10^3$ Nmm = 0,165 kNm

From figure 22 it can be learned that the moment resistance to the strengthened walls is much greater. This is due to the application of elements that can resist tensile stress and/or forces. These elements are:

- CFRP-strips
- cement-matrix finishing with CFRP-net
- polymer based finishing

The tensile resistances and its relation to deformations is described in paragraph 2.1 from this it is concluded that although the capacity of the CFRP-strips is rather high, due to the application of the Q-poxy the CFRP-strips are not so stiff. Hereafter the tensile capacity and the bond behaviour is described.

Although the CFRP-net has a tensile capacity that is significantly higher than the tensile capacity of the cement-matrix finishing on paper, the failure mechanism of the tested specimens shows that the CFRP-net fails directly or shortly after failure of the cement-matrix finishing. Therefore, the tensile capacity of specimens with a cement-matrix finishing with an embedded CFRP-net will be based on the tensile capacity of the cement-matrix:

$F_t = A_{c.layer}\ f_{ct} = 15 \cdot 650 \cdot 5 = 48{,}7 \cdot 10^3$ N = 48,7 kN

The thickness of the polymer finishing is approximately 5 mm. The tensile strength of the material is 45 N/mm². The tension capacity for the specimens with a polymer finishing follows from:

$F_t = A_{p.layer}\ f_{pt} = 5 \cdot 650 \cdot 45 = 146 \cdot 10^3$ N = 146 kN

2.3 Structural behaviour of QSS+ specimens

The bond behaviour of the CFRP-strips and the behaviour of the specimen is so that it is chosen to describe the structural behaviour of the QSS+ specimen in a discrete way as shown in figure 24. It is assumed that during the test, the specimen consists of three stiff masonry blocks and that the deformation of the specimen is the result of the deformation in the joints between the three blocks. The deformation of the specimen is determined by the behaviour of the two discrete cracks rather than the smooth curvature of the masonry.

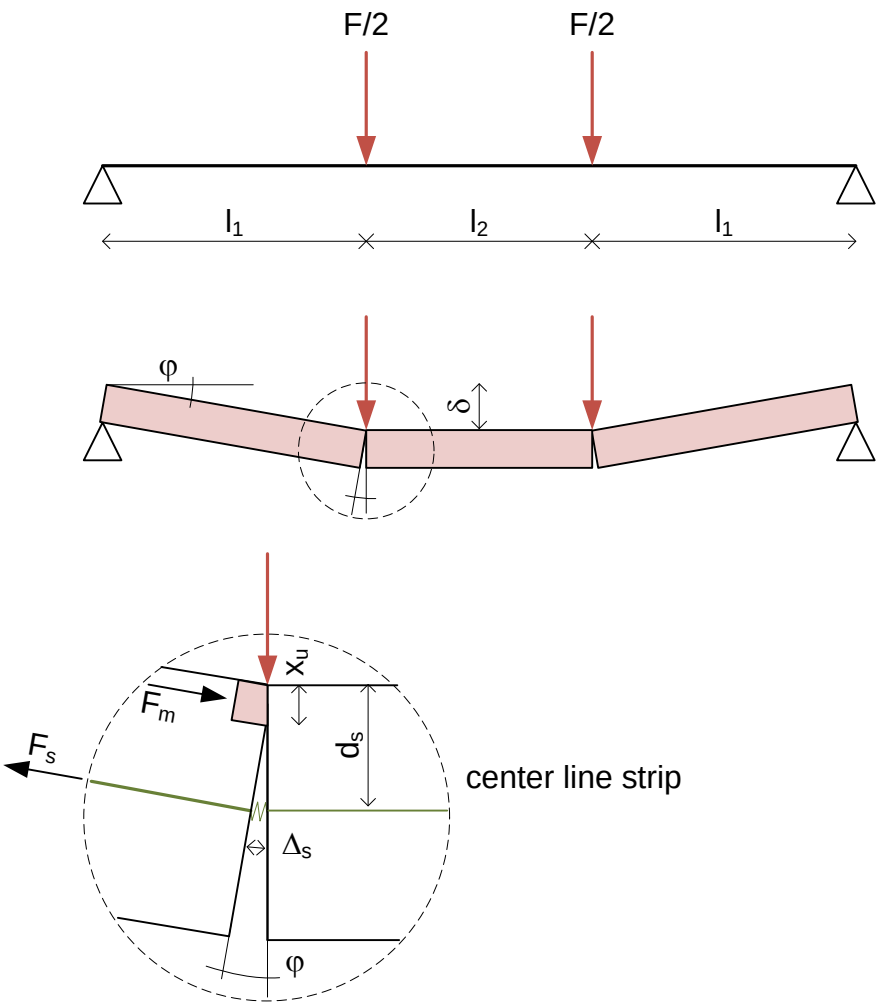

figure 24 Model for structural behaviour of the QSS specimen

The moment in the joint is the result of a compression force in the top of the stiff masonry block, the tension force in the spring which represent the CFRP-strip and the lever arm between the two forces. The distance between the centre line of the strip and the edge of the masonry on the compression side, is considered as the effective depth of the section, d_s. It is assumed that the lever arm, z, equals the effective depth minus half of the assumed depth of the compression zone x_u:

$$z = d_s - \frac{x_u}{2}$$

Due to presence of n_s number of strips in the joint the internal moment follows from:

$$M = n_s F_s z$$

The rotation in the joint is the result of displacement difference between the strip and the masonry due to force F_{strip} divided by the distance between the centre line of the strip and the assumed neutral axis:

$$\varphi = \frac{\Delta_s}{d_s - x_u}$$

The relation between the rotation in the joint and the displacement at the midspan of the specimen follows from:

$$\delta = \varphi\, l_1$$

The internal moment in the joint should equal the external moment in the joint, so the relation between the external load F and the moment in the joint follows from:

$$F = \frac{2M}{l_1}$$

From these equations, for a given displacement at midspan, the relation with the external load F can be found:

$$\varphi = \frac{\delta}{l_1}$$

$$\Delta_s = \varphi\,(d_s - x_u)$$

Where Δ_s is the slip of the strip in the end block. Because the force in the strip in the mid block is constant, no slip will occur in the mid block. From Δ_s the value for q_s can be derived from the following relation:

$q_s = 15\,\Delta_s$	when $\Delta_s \leq 3$ mm
$q_s = 45 + 5(\Delta_s - 3)$	when 3 mm $< \Delta_s \leq 4$ mm
$q_s = 50 - 5{,}7(\Delta_s - 4)$	when 4 mm $< \Delta_s \leq 7$ mm
$q_s = 0$	when 7 mm $< \Delta_s$

From the embedded length l_{em} and q_s the force in one strip can be found:

$$F_s = q_s\, l_{em}$$

From this the external load can be found:

$$F = \frac{2M}{l_1} = \frac{2 n_s F_s z}{l_1}$$

For the given variables of the QSS+ specimens:

distance between support and load point:	$l_1 = 430$ mm
embedded length of the strip:	$l_{em} = 505$ mm
thickness of the wall:	$t = 101$ mm
effective height in the cross section	$d_s = 50$ mm
number of strips in the wall	$n_s = 2$
assumed depth of the compression zone	$x_u = 12$ mm

and the described relation between q_s and Δ_s,

the relation between the external load F and the midspan deflection δ can be found, see figure 25.

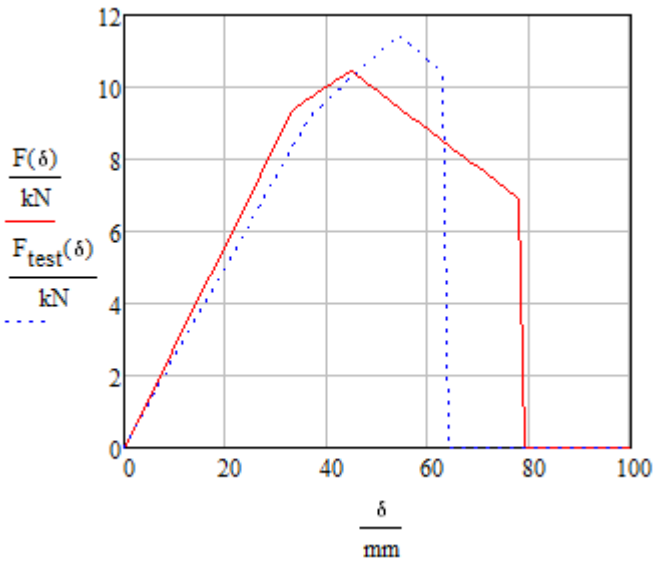

figure 25 Relation between external load F and displacement δ for QSS+

A comparison with the graph in figure 7, of which F_{test} is plotted in the figure, shows that the chosen model results in a good description of the structural behaviour of the QSS+ specimens.

The maximum tensile force in the strip equals 50 l_{em} = 50·505 = 25,3·10^3 N

The maximum compression force in the masonry is, due to the presence of two strips, equal to 50,6 kN. From the assumption of the depth of the compression zone of 12 mm the compressive stress in the masonry can be calculated:

$$\sigma_{cm} = \frac{50{,}6 \cdot 10^3}{12 \cdot 650} = 6{,}5 \text{ N/mm}^2$$

This compressive stress is smaller than the compressive strength of 7,1 N/mm², the assumption that the depth of the compression zone can equal 12 mm is valid.

2.4 Structural behaviour of QSS- specimens

The structural components in the QSS- specimens are identical to those in the QSS+ specimens. However from figure 22 it shows that the capacity and the stiffness of these specimens are significant smaller than those of the QSS+ specimens. An explanation for this can be found in two circumstances:

- the quality of the masonry on the compression side, which for the QSS- specimens is the construction side, is poor due to the incomplete filling of the bed joints;
- the position of the CFRP-strips can be a little bit higher than assumed, due that the strips are pressed into the Q-poxy from the construction side.

From this, for the QSS-specimens it is chosen that the effective depth equals 40 mm instead to 50 mm. Taken this into account the force-displacement relation as described in figure 26 is found.

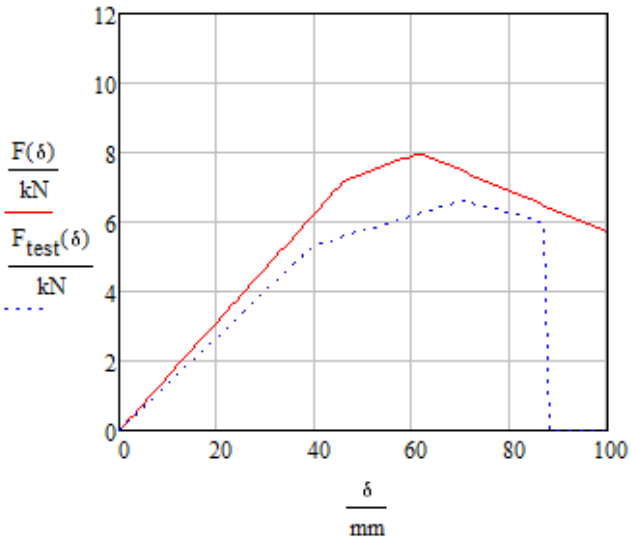

figure 26 Relation between external load F and displacement δ for QSS-

A comparison with the graph in figure 10 shows that, however the maximum load is slightly higher, the chosen model results in a relatively good description of the structural behaviour of the QSS- specimens

2.5 Structural behaviour of QSP+ specimens

From figure 22 it shows that both the capacity and the stiffness of the QSP+ is higher than those of the QSS+ specimens. In the specimens there is an additional structural element: the polymer based finishing which has a tensile capacity. This makes that the previous model has to be adjusted. This is done by extending the discrete model with an additional spring that describes the structural properties of the polymer based finishing in the joint as shown in figure 27.

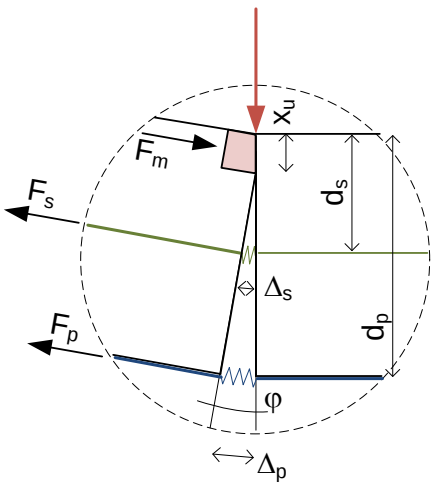

figure 27 Model for structural behaviour of the QSP+ specimen

Due to the fact that the polymer finishing follows the surface of the masonry and therefor is not straight and flat, the stiffness of the spring can not be derived from the mechanical properties of the polymer and an assumption has to be made. It is assumed that this spring behaves linear until a certain elongation Δ_p and that after that point the force in the finishing reduces. Based on fitting to the results of the external force displacement relation of the QSP+ specimens the following relation between the deformation and the force is used for the specimens with a width of 650 mm:

$F_p = 1300\ \Delta_p$	when $\Delta_p \leq 12$ mm
$F_p = 23400 - 650\ \Delta_p$	when 12 mm $< \Delta_p \leq 17$ mm
$F_p = 0$	when $\Delta_p > 14$ mm

The relation between F_p and Δ_p is presented in the graph in figure 28.

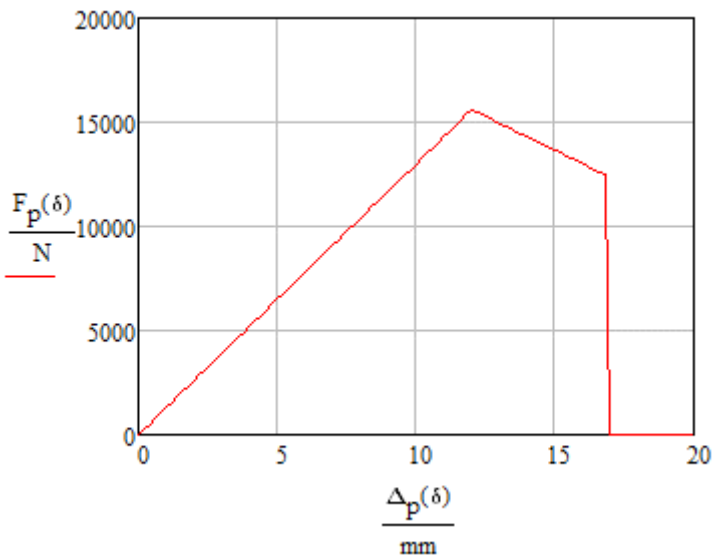

figure 28 Relation between Δ_p and F_p

The relation between the deformation of the CFRP-strips Δ_s and the polymer finish Δ_p is linear to the relation between the distance between the particular elements and the neutral axis:

$$\Delta_p = \Delta_s \frac{d_p - x_u}{d_s - x_u}$$

The moment in the joint follows from:

$$M = n_s F_s z_s + F_p z_p$$

where:

$$z_s = d_s - \frac{x_u}{2}$$

$$z_p = d_p - \frac{x_u}{2}$$

The rotation in the joint can be derived from the difference between the elongation of the strip and the surrounding masonry and its position in the cross section:

$$\varphi = \frac{\Delta_s}{d_s - x_u}$$

The relations between the rotation in the joint and the displacement at midspan and the relation between the external load F and the moment in the joint are as described previous.

From these equations, for a given displacement at midspan, the relation with the external load F can be found:

$$\varphi = \frac{\delta}{l_1}$$

$\Delta_s = \varphi\ (d_s - x_u)$
$\Delta_p = \varphi\ (d_p - x_u)$

From Δ_s the value for q_s can be derived from the known nonlinear relation:

$q_s = 15\ \Delta_s$	when $\Delta_s \leq 3$ mm
$q_s = 45 + 5(\Delta_s - 3)$	when 3 mm $< \Delta_s \leq 4$ mm
$q_s = 50 - 5{,}7(\Delta_s - 4)$	when 4 mm $< \Delta_s \leq 7$ mm
$q_s = 0$	when 7 mm $< \Delta_s$

From the embedded length l_{em} and q_s the force in one strip can be found:

$$F_s = q_s\ l_{em}$$

From Δ_p the force in the polymer finishing F_p can be derived as described previous.

From this the external load can be found:

$$F = \frac{2M}{l_1} = \frac{2}{l_1}\ (\ n_s\ F_s\ z_s + F_p\ z_p)$$

For the given variables of the QSP+ specimens:
l_1 = 430 mm
l_{em} = 505 mm
t = 101 mm
d_s = 50 mm
n_s = 2
an assumed x_u = 15 mm
and the described relations between q_s and Δ_s and F_p and Δ_p the following relation between external load F and displacement δ is found.

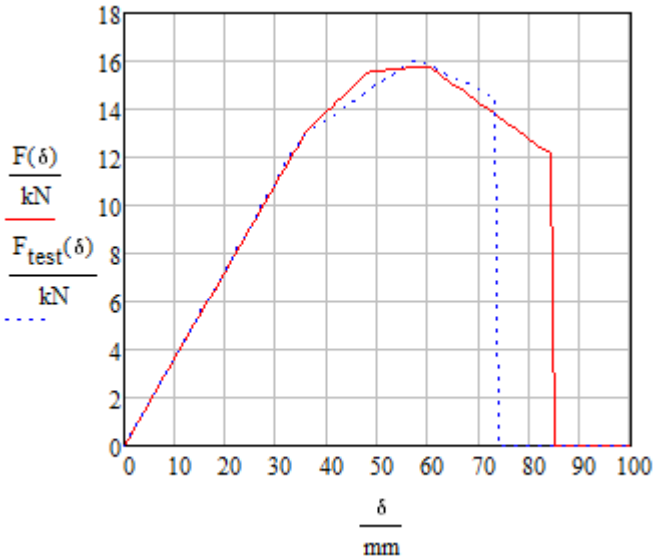

figure 29 Relation between external load F and displacement δ for QSS+

A comparison with the graph in figure 7, of which the load is shown in the graph as $F_{test,}$ shows that the chosen model results in a good description of the structural behaviour of the QSP+

The maximum tensile force in the combination of strips and poly finishing is found when the tensile force in the strip is maximum:

$\Delta_s = 4$ mm	$n_s F_s =$	50,6 kN
$\Delta_p = \Delta_s (d_p - x_u)/(d_s - x_u) = 4 \cdot 85/35 = 9{,}7$	$F_p = 1300 \cdot 9{,}7 =$	12,6 kN
	$n_s F_s + F_p =$	63,2 kN

The maximum compression force in the masonry is equal to 63,2 kN. From the assumption of the depth of the compression zone the compressive stress in the masonry can be calculated by assuming a rectangular stress block:

$$\sigma_{cm} = \frac{63{,}2 \cdot 10^3}{15 \cdot 650} = 6{,}5 \text{ N/mm}^2$$

This compressive stress is smaller than the compressive strength of the masonry (7,1 N/mm²), the assumption that the masonry is able to withstand the tensile force in the CFRP-strips is valid.

2.6 Structural behaviour of QSP-

As shown in table 3 the QSP- configuration is not tested. In the QSP- configuration the polymer finishing is present on the compression side. It is assumed that due to the difference in Young's modulus between masonry and the polymer finishing, the polymer finishing will not have a significant contribution in withstanding the compression force in the cross section. There the structural behaviour of the QSP- configuration will be similar to the behaviour of the QSS configurations.

2.7 Structural behaviour of QSC+ specimens

2.7.1 Introduction

In comparison to the QSS specimens, in the QSC+ specimens there is an additional structural element: the cement-matrix with a CFRP-net finishing, which has a tensile capacity. It is this element that causes the different behaviour of the QSC+.

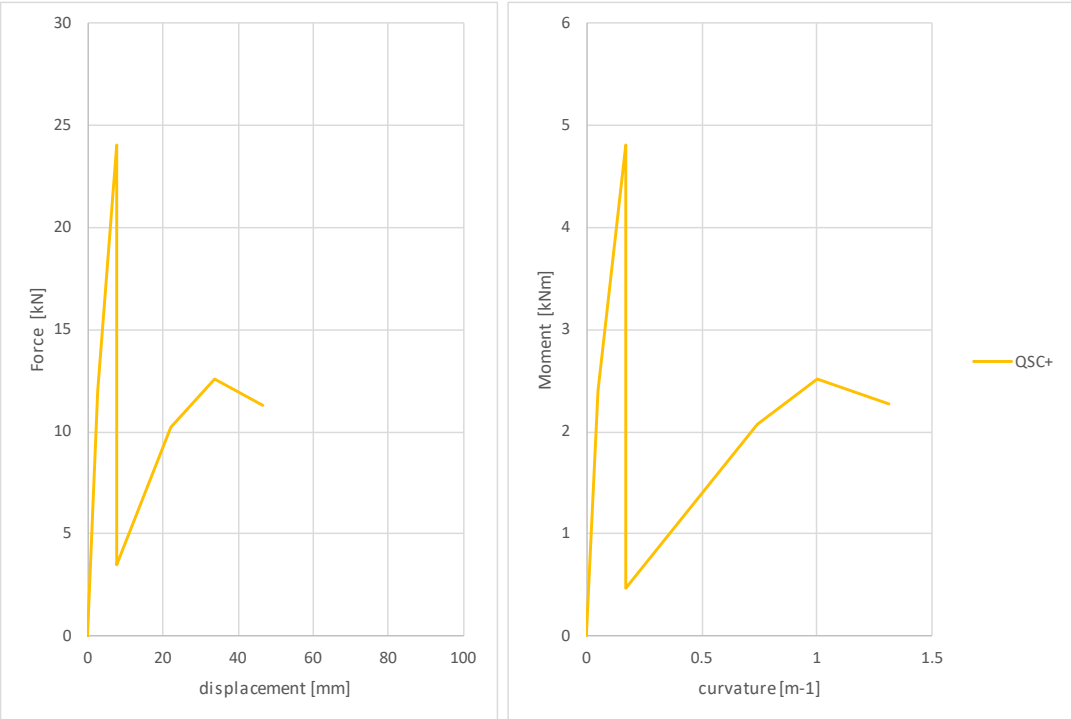

figure 30 Average of force-displacement and moment-curvature behaviour QSC+

Due to the tensile capacity of the reinforced cement matrix the resistance against an external load is greater. In the tests the maximum external load, with a mean value of approximately 24 kN, is reached in two steps, see figure 30. With the used setup, see figure 15, the maximum moment can be calculated as follows:

$M_{max} = M_2 = ¼\ F_2\ L = ¼\ 24 \cdot 0{,}8 = 4{,}8$ kNm

It should be noted that the moment resistance of the masonry without QuakeShield strengthening equals:

$M_{masonry} = f_{mt}\ W = 0{,}15 \cdot 650 \cdot 100^2/6 = 0{,}16 \cdot 10^6$ Nmm = 0,16 kNm.

Hereafter the behaviour of the specimen is described for the two different peaks. De description of the first peak is based on the tensile strength and deformation of the cement-matrix finish. Due to the small deformations, the polymer strips will not influence the behaviour of the specimen. The description of the second peak is based on the model as discussed for the previous described specimens.

2.7.2 First peak behaviour

The behaviour up until the first peak is presented in figure 16. The force-displacement relation is linear until an external force of 12 kN. The corresponding displacement is 2,5 mm. After that a further load increase is possible to 24 kN with a corresponding displacement of 7,5 mm.

From the load scheme and the force-displacement relation a moment-curvature relation is derived.

$M_1 = ¼\ F_1\ L = ¼\ 12 \cdot 0{,}8 = 2{,}4$ kNm $\qquad \kappa_1 = 0{,}05\ m^{-1}$
$M_2 = ¼\ F_2\ L = ¼\ 24 \cdot 0{,}8 = 4{,}8$ kNm $\qquad \kappa_1 = 0{,}17\ m^{-1}$

This moment-curvature relation is approximated by considering the following stress-strain relations for the masonry and the reinforced cement-matrix in the section.

Masonry:

mean compressive strength	f_{cm} = 7,00 N/mm²
mean flexure strength with a failure plane parallel to the bed joint	f_{xm} = 0,15 N/mm²
mean Youngs modulus	E_m = 2000 MPa

Reinforced cement-matrix
$f_{ct.1}$ = 3 MPa $\qquad \varepsilon_{ct.1}$ = 0,004
$f_{ct.2}$ = 5 MPa $\qquad \varepsilon_{ct.2}$ = 0,016

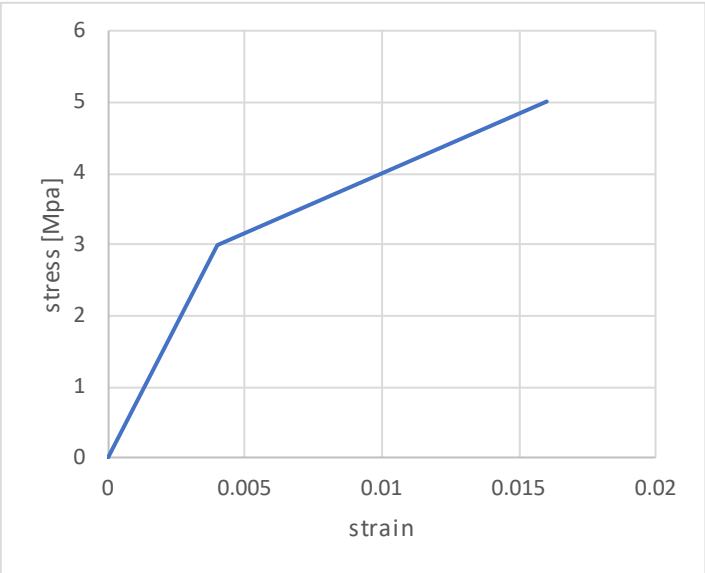

figure 31 Stress-strain relation reinforced cement-matrix under tension

These stress-strain relations, combined with a masonry thickness of 100 mm and a cement-matrix thickness of 15 mm result in the moment-curvature relations as shown in figure 32.

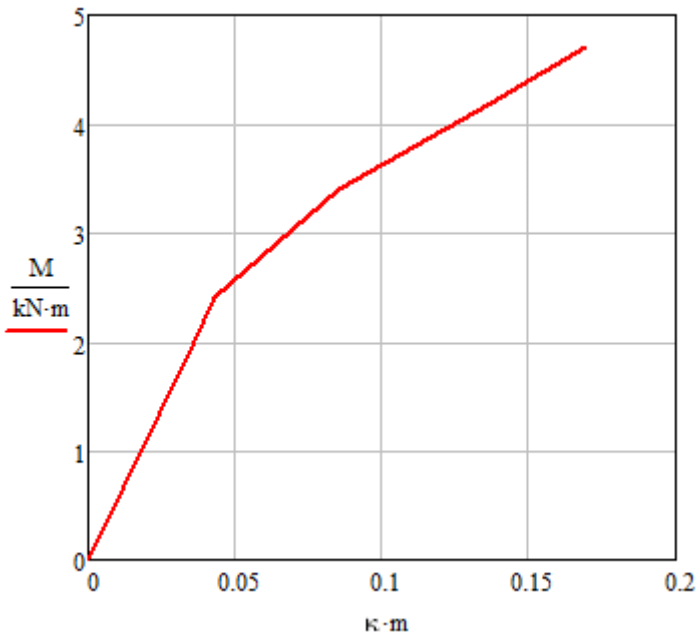

figure 32 Moment-curvature relation for QSC+ first peak

As a simplified approach the ultimate moment resistance and the ultimate curvature can be calculated from the following approach:

The maximum tensile force in the reinforced cement-matrix follows from:
F_{ct}= b t_c f_{ct} = 650·15·5 = 48,7·10^3 N

The depth of the compression zone in the masonry can be approximated by:
x = 2F_{ct}/(b f_m) = 2·48,7·10^3/(650·7) =21,4 mm

The moment resistance results from:
z = t_m – x/3 + t_c/2 = 100 – 21,4/3 + 15/2 = 100 mm
M_R = F_{ct} z = 48,7·0,1 = 4,8 kNm

The ultimate curvature can be calculated from:
$\kappa_R = \varepsilon_{ct.2}/(t_t - x)$ = 0,016/(0,115 – 0,020) = 0,17 m^{-1}

Based on the ultimate moment resistance the maximum load on the specimen follows from the following equation:
F = 4 M_R /L = 4·4,8/0,8 = 23,5

When a full linear relation between moment and curvature is assumed the maximum deflection of the specimen can be derived from the following equation:

$\delta = \kappa_R L^2/12$ = 0,17·0,8²/12 = 0,009 m = 9 mm

This a small overestimation of the deflection, which equals 7,5 mm. This can be explained by the effect that in case of small moments, a cross section reacts relatively stiff. Also, the fact that the

CEM-layer continues over the supports in the used test set-up, may contribute to this effect. To take into account the slightly stiffer behaviour, the deflection will be calculated from the following equation:

$\delta = \kappa_R L^2/15 = 0{,}17 \cdot 0{,}8^2/15 = 0{,}0073$ m = 7,3 mm

The previous described model is sketched in the figure below.

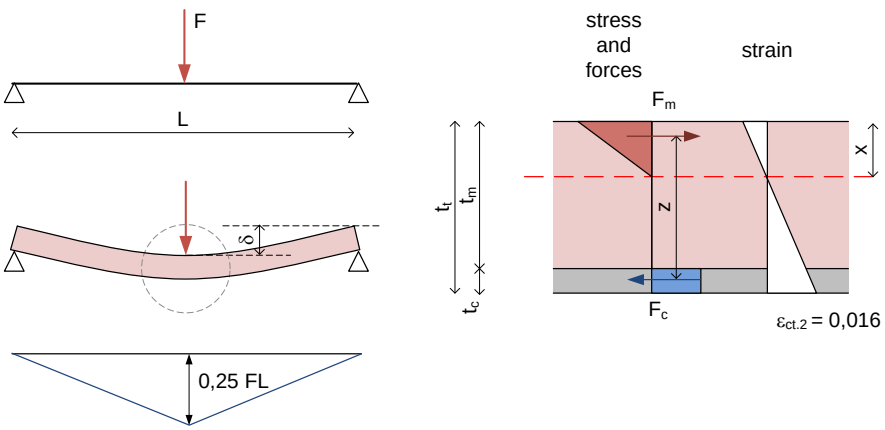

figure 33 Model for behaviour based on reinforced cement-matrix

2.7.3 Second peak behaviour

After the first peak resistance is past, the QSC+ specimens behave like the QSS+ specimens. Off course the stiffness of the specimen will be larger due to the finishing but, in the assumed model with the joint and the stiff masonry blocks, this higher stiffness will not have such a big influence.

The appearance of brittle failure in the first two tests is not of big concern. The failure will be caused by a flexural shear crack in a section where the stiff and strong finishing has been stopped and the support is still at a distance of approximately 100 mm. Such a section is not present in practice.

Because the setup of the test is changed from a four point bending test to a three point bending test, the model as described in 2.3 has to be adjusted slightly.

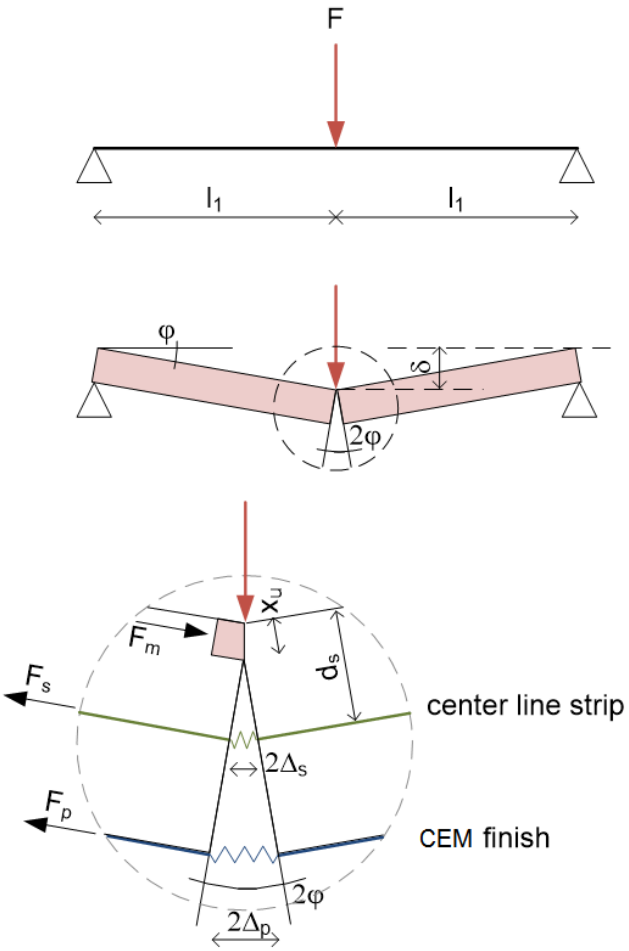

figure 34 Model for structural behaviour of the QSC+ specimen in a three point bending test

The equations as presented in paragraph 2.3 are repeated without explanation, unless it has been changed.

$$z_s = d_s - \frac{x_u}{2}$$

$$M = n_s F_s z_s$$

$$\varphi = \frac{\Delta_s}{d_s - x_u}$$

$$\delta = \varphi l_1$$

$$F = \frac{2M}{l_1}$$

From these equations, for a given displacement at midspan, the relation with the external load F can be found:

$$\varphi = \frac{\delta}{l_1}$$

$$\Delta_s = \varphi\,(d_s - x_u)$$

From Δ_s the value for q_s can be derived from the following relation:

$q_s = 15\,\Delta_s$	when $\Delta_s \leq 3$ mm
$q_s = 45 + 5(\Delta_s - 3)$	when 3 mm $< \Delta_s \leq 4$ mm
$q_s = 50 - 5{,}7(\Delta_s - 4)$	when 4 mm $< \Delta_s \leq 7$ mm
$q_s = 0$	when 7 mm $< \Delta_s$

From the embedded length l_{em} and q_s the force in one strip can be found:

$$F_s = q_s\, l_{em}$$

From this the external load can be found:

$$F = \frac{2\, n_s F_s z}{l_1}$$

For the given variables of the QSC+ specimens:
l_1 = 400 mm
l_{em} = 625 mm
t = 101 mm
d = 50 mm
n_s = 2
an assumed x_u = 15 mm
and the described relation between q_s and Δ_s, the relation between the external load F and the mid-span deflection δ can be found, see figure 35.

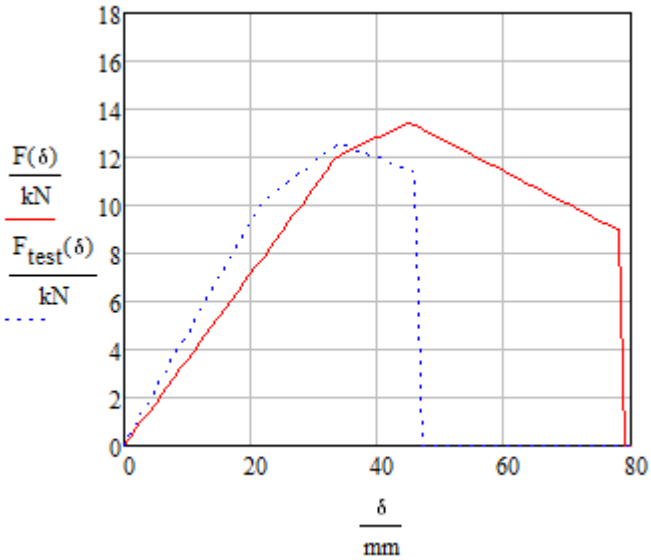

figure 35 Relation between external load F and displacement δ for QSC+

A comparison with the graph of the second peak in figure 30, of which the result is plotted as F_{test}, shows that the chosen model results in a good description of the structural behaviour of the QSC+ specimens as far as the stiffness and the capacity is considered.

The maximum tensile force in the strip equals 50 l_{em} = 50·625 = 31,3·10^3 N

The maximum compression force in the masonry is, due to the presence of two strips, equal to 62,6 kN. From the assumption of the depth of the compression zone of 15 mm the compressive stress in the masonry can be calculated:

$$\sigma_{cm} = \frac{62{,}6 \cdot 10^3}{15 \cdot 650} = 6{,}4 \text{ N/mm}^2$$

This compressive stress is smaller than the compressive strength of 7,1 N/mm², so the assumption that the depth of the compression can equal 15 mm is valid.

2.8 Structural behaviour of QSC- specimens

In the QSC- configuration, the cement-matrix layer is on the compression side of the specimen. The compressive strength of the cement-matrix is greater than that of the masonry. Also the less good quality of the masonry specimens on the compression side, as discussed in paragraph 2.4 for the specimens QSS- is compensated by the application of the cement-matrix finishing on the construction side of the specimens. Therefore it can be assumed that the compression force, as described in the model, can be resisted by the cement-matrix and that the effective depth of the CFRP-strip is increased with 15 mm and the depth of the compression zone can be reduced.

From this, for the QSC-specimens the force-displacement relation as described in figure 36 is found.

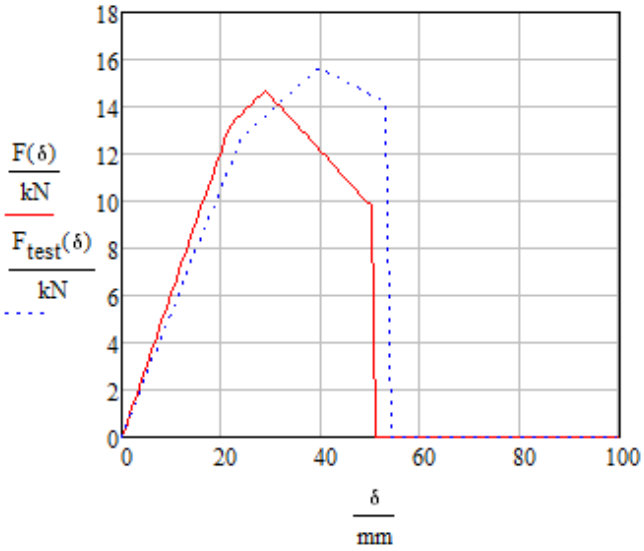

figure 36 Relation between external load F and displacement δ for QSC-

A comparison with the results of the experimental research of which the result is plotted as F_{test}, shows that the chosen model results in a good description of the structural behaviour of the QSC-specimens.

2.9 Adjustment of the model for the presence of axial loads and variable width

2.9.1 General

The described models, that can be used for a nonlinear push over calculation, easily can be adjusted for the presence of an axial load. First this is shown for the model that describes the behaviour of the wall when it is determined by the slip of the polymer strip and with one extreme moment, equal to that of the three point bending test as described in 2.7.3. Thereafter the behaviour is described in case the tension capacity is provided by the reinforced cement-matrix as described in 2.7.2.

2.9.2 Capacity based on polymer strips

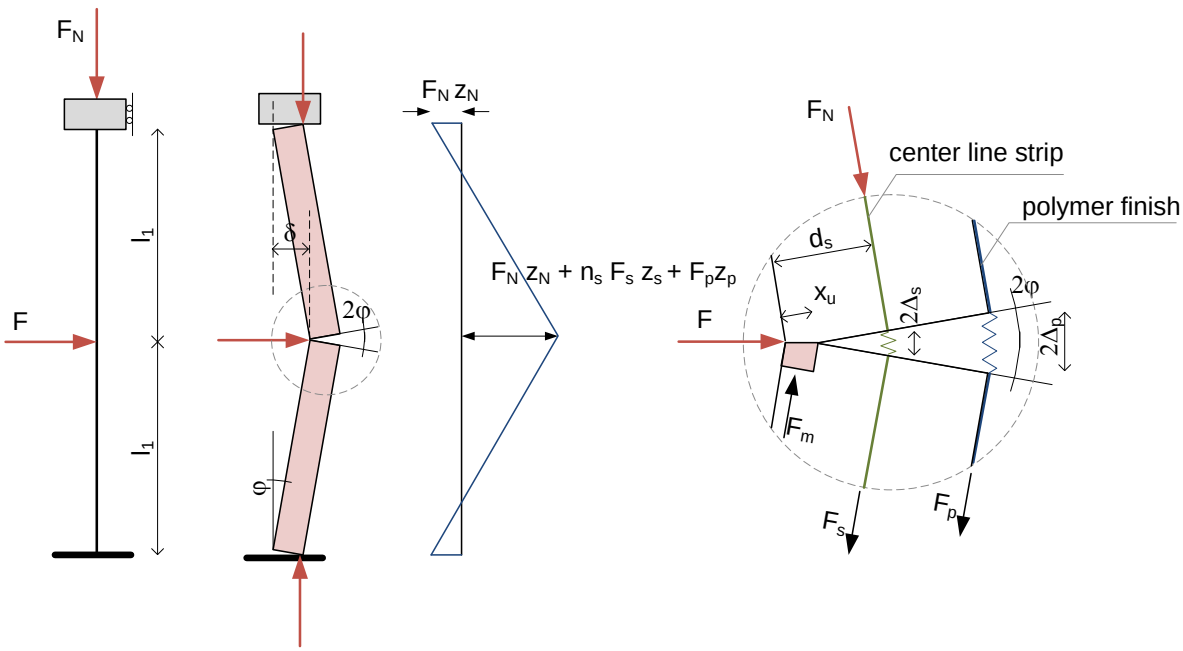

figure 37 Model for structural behaviour of specimen in a three point bending test

The depth of the compression zone is determined based on the axial load, the maximum load in the strips and the average compression strength of the masonry. The maximum load in the strips follows from:

$$F_{s,max} = l_{em}\, q_{s,max}$$

$$x_u = \frac{F_N + n_s F_{s,max}}{b\, f_m}$$

where:

l_{em} is the embedded length;
$q_{s,max}$ is the maximum bond force, equal to 50 N/mm;
n_s is the number of strips;
b is the width considered;
f_m is the mean compressive strength of the masonry.

For a given displacement at midspan, the relation with the external load F can be found:

$$\varphi = \frac{\delta}{l_1}$$

$\Delta_s = \varphi\ (d_s - x_u)$

From Δ_s the value for q_s can be derived from the following relation:

$q_s = 15\ \Delta_s$	when $\Delta_s \leq 3$ mm
$q_s = 45 + 5(\Delta_s - 3\text{ mm})$	when 3 mm $< \Delta_s \leq 4$ mm
$q_s = 50 - 5{,}7(\Delta_s - 4\text{ mm})$	when 4 mm $< \Delta_s \leq 7$ mm
$q_s = 0$	when 7 mm $< \Delta_s$

where:
q_s is the bond force per unit of length [N/mm];
Δ_s is the displacement difference between strip and masonry [mm].

From the embedded length l_{em} and q_s the force in one strip can be found:

$F_s = q_s\ l_{em}$

The force in the strip should be limited to its capacity. For the standard strips 20×1,4 mm² this equals 78,5 kN. This capacity will be reached when the embedded length equals 1,57 m. The deformation capacity is limited to the point the capacity of the strips is reached.

The tensile force in the polymer finish is related to the elongation of the polymer finish Δ_p:

$F_p = 2\ b\ \Delta_p$	when $\Delta_p \leq 12$ mm
$F_p = b\ (36\text{ mm} - \Delta_p)$	when 12 mm $< \Delta_p \leq 17$ mm
$F_p = 0$	when $\Delta_p > 17$ mm

where:
F_p is the tensile force in the polymer finish [N];
b is the width of the wall [mm];
Δ_p is the elongation of the polymer finish [mm].

The sum of the internal moment equals:

$$\Sigma M_{int} = 2F_N\ z_N + n_s F_s \left(d_s - \frac{x_u}{2}\right) + F_p \left(d_p - \frac{x_u}{2}\right)$$

where:
z_N is the distance between the centre of the cross section and the point of gravity of the compression force in the masonry.

It is obvious that when the displacement δ is equal to 0, the point of gravity of the compression force in the masonry is in the centre of the cross section, so z_N equals 0. In the model it is assumed that z_N increases linear from 0 to $\frac{t - x_u}{2}$ when Δ_s increases from 0 to 1 mm. After this z_N remains constant, so:

$$z_N = \frac{t - x_u}{2} \frac{\Delta_s}{1\text{mm}} \qquad \text{when } \Delta_s \leq 1\text{ mm}$$

$$z_N = \frac{t - x_u}{2} \qquad \text{when } \Delta_s > 1 \text{ mm}$$

The variable that determine ΣM_{int} are related to δ and an assumed value for x_u.

The sum of the external moment equals:

$$\Sigma M_{ext} = ½ F l_1 + F_N \delta$$

Because the sum of the internal moment and the external moment should be equal, from this the relation between the external load and the displacement δ can be found.

As can be seen in the previous equations, the axial load F_N influences both the internal moment en the external moment. When the displacement δ is greater than $2z_N$, due to the second order effect, the presence of the axial load will reduce the value of the horizontal load F. From this it can be considered to limit the displacement capacity of the wall when the behaviour factor is determined. By doing so the reduction on the seismic effected will be limited but also the second order effect will be smaller and in combination the resistance against a seismic effect can be greater.

2.9.3 Capacity based on reinforced cement-matrix

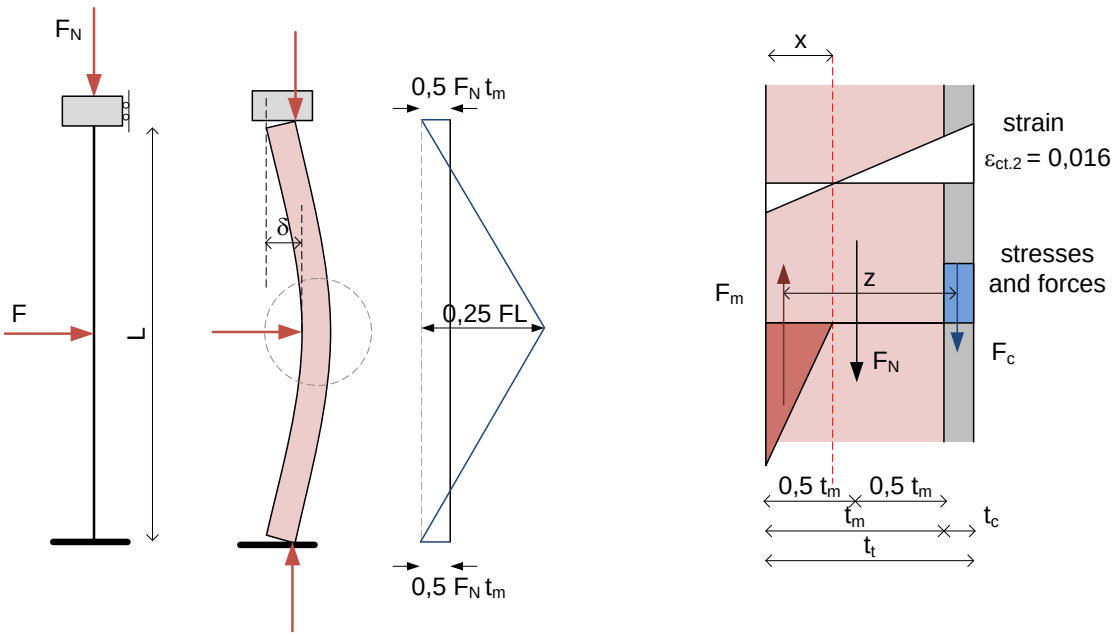

figure 38 Model for structural behaviour of specimen in a three point bending test

Due to the fact that the displacement capacity of the masonry wall with a cement-matrix finishing is limited, the second order effect of the displacement and the axial load is neglected.

The properties of the reinforced cement-matrix are summarized hereafter:
f_{ct} = 5 MPa
$\varepsilon_{ct.u}$ = 0,016

The maximum tensile force in the reinforced cement-matrix follows from:
$F_{ct} = b\ t_c\ f_{ct}$

The depth of the compression zone in the masonry can be approximated by:
$x = 2(F_{ct} + F_N)/(b\ f_m)$

The moment resistance results from:
$z_c = t_m - x/3 + t_c/2$
$z_N = t_m/2 - x/3$
$M_R = F_{ct}\ z_c + F_N\ z_N$

The ultimate curvature can be calculated from:
$\kappa_R = \varepsilon_{ct.u}/(t_t - x)$
Based on the ultimate moment resistance the maximum horizontal load on the specimen follows from the following equation:

$$F = \frac{4}{L}\left(M_R + F_N \frac{t_m}{2}\right)$$

Based on the distribution of the moment at extreme loading and the known curvature the maximum displacement can be estimated as:

$$L_m = L \frac{M_R}{M_R + F_N \frac{t_m}{2}}$$

$$\delta = \kappa_R\ L\ L_m/15$$

From the known force and displacement a linear relation between the force and displacement can be derived.

2.10 Conclusion and summary

In the previous paragraphs two models to describe the structural out of plane behaviour of masonry walls which are strengthened with the QuakeShield system are presented. The first model, where the capacity is derived from the polymer strips, consists of stiff masonry blocks and discrete joints at the locations of the maximum moment. The relation between the internal moment and the rotation in the joint is based on the bond behaviour of the CFRP-strips and, when it is applied, the polymer finish. The tensile capacity of the finish consisting of the cement-matrix and the CFRP-net is not taken into account.

The results of the model, especially where the influence of the CFRP-strips are considered, are compared to the results of the performed experimental research that is described in [2]. It shows that the bond behaviour of these strips, derived from [1] considered in the model, describes the behaviour of the strengthened masonry panels quite well. The description of the bond behaviour of the polymer finish is based on fitting of the results of [2].

The second model, where the capacity is based on the tensile capacity of the reinforced cement-matrix, describes for the specimens QSC+ a much stiffer behaviour. In this model the deformations

are the result of the curvature that occurs in the cross sections of the wall. Due to the fact that in this model the displacements are much smaller here the second order effects are not considered.

3 Determination of the design value of the resistance

In table 3.12 of [2] the coefficient of variation of the moment capacity of the several configurations is presented. The values are presented hereafter:

table 4 number of tests and coefficients of variation for the configurations tested in [2]

configuration	QSS+	QSS-	QSP+	QSC+	QSC-
n	10	11	11	10	11
V_x	0,092	0,262	0,085	0,143	0,114

It shows that the coefficient of variation for the QSS- configuration is rather high compared to the other values. This is discussed already in paragraph 2.4. The quality of the masonry work is so, that here it is chosen not to consider this coefficient of variation.

The average value of the other coefficient of variation equals 0,11. The number of tests of the 4 configurations considered is 42. The coefficient k, to determine the characteristic value with a 5% failure change can be taken an 1,7 (Annex D of NEN-EN 1990).

The mean value of the moment capacity can be determined with the model described in section 2 of this report. The characteristic value follows from:

$M_k = M_m (1 - 1{,}7 \cdot 0{,}11) = 0{,}81\ M_m$

The design value of the moment have to be determined according 4.4.2.2 of NPR 9998:

$$M_d = \frac{M_k}{\gamma_m \gamma_M}$$

where:
γ_m = 1,5
the value according section 9 of the NPR 9998
γ_M follows from table 2.1 or table 2.2 of the NPR 9998.

The variable γ_m is a partial factor used to describe the degeneration of the structure due to the cyclic loading will the variable γ_M is a partial factor to create an sufficient reliability of the structure.

4 Procedure to verify out of plane behaviour in seismic conditions

4.1 General

The procedure to verify the out of plane behaviour of a masonry wall strengthened with the QuakeShield system is based on NPR 9998 and the note 2-12-2015 ‘Metselwerk wanden belast uit

het vlak' by Adviesbureau Hageman. According to these documents, the following steps have to be performed:

1. In both directions of the out of plane behaviour a nonlinear push-over calculation has to be performed, using the models described in section 2 of this report;
2. Based on the result of these push-over calculations the natural period T and the behaviour factor q have to be determined;
3. Given the design spectrum, T and q the equivalent static out of plane load can be determined;
4. The effect of the static equivalent load has to verified against the design value of the capacity.

4.2 Example calculation A

Hereafter an example of a load bearing wall is presented. The calculation is performed as a calculation in which a chosen design is checked. The calculation is performed for a QSS type wall.

Input for the calculation

height of the wall	$l = 2500$ mm
width of the wall	$b = 1000$ mm
thickness of the wall	$t = 100$ mm
number of strips per width	$n_s = 2{,}7$
effective depth of the strips	$d_s = 50$ mm
axial load on the wall	$F_N = 18$ kN
unit mass of masonry	$\gamma = 1800$ kg/m³
mean compressive strength	$f_m = 9{,}9$ N/mm²
peak ground acceleration	$a_{g,ref} = 0{,}2$ g
factor for design value pga	$k_{ag} = 1{,}4$
partial factor for resistance	$\gamma_M = 1{,}1$

Nonlinear push-over calculation

$l_1 = l/2 = 1250$ mm

$l_{em} = l_1 = 1250$ mm

$F_{s.max} = l_{em}\, q_{s,max} = 1250 \cdot 50 = 62{,}5 \cdot 10^3$ N

$$x_u = \frac{F_N + n_s F_{s,max}}{b\, f_m} = \frac{18 \cdot 10^3 + 2{,}7 \cdot 62{,}5 \cdot 10^3}{1000 \cdot 9{,}9} = 18{,}9 \text{ mm}$$

The rotation φ can be expressed as a function of the displacement δ:

$$\varphi(\delta) = \frac{\delta}{l_1}$$

From this also the slip of the strip Δ_s can be expressed as a function of δ:

$$\Delta_s(\delta) = \varphi(\delta)\,(d_s - x_u)$$

From Δ_s the value for the bond force q_s can be derived from the following relation:

$q_s = 15\ \Delta_s$	when $\Delta_s \leq 3$ mm
$q_s = 45 + 5(\Delta_s - 3\text{ mm})$	when $3\text{ mm} < \Delta_s \leq 4$ mm
$q_s = 50 - 5{,}7(\Delta_s - 4\text{ mm})$	when $4\text{ mm} < \Delta_s \leq 7$ mm
$q_s = 0$	when $7\text{ mm} < \Delta_s$

and therefor can be expressed as a function of δ.

From the embedded length l_{em} and q_s the force in one strip can be found:

$F_s(\delta) = q_s(\delta)\ l_{em}$

The force in the strip should be limited to its capacity. For the standard strips 20×1,4 mm² this equals 78,5 kN. This capacity will be reached when the embedded length equals 1,57 m. In this case the embedded length is smaller so failure of the strip is not expected.

The internal lever arm of the axial force, z_N, which is active both at the connection with the floors and at midspan, is depending on Δ_s and therefor depending on the displacement δ:

$$z_N(\delta) = \frac{t - x_u}{2}\frac{\Delta_s(\delta)}{1\text{mm}} \qquad \text{when } \Delta_s(\delta) \leq 1\text{ mm}$$

$$z_N(\delta) = \frac{t - x_u}{2} \qquad \text{when } \Delta_s(\delta) > 1\text{ mm}$$

For the wall considered the sum of the internal moment capacity is determined. Due to the expected great displacements, it is assumed that for both intermediate walls and for end walls the moment capacity at the end of the wall equals $F_N\ z_N$ at both ends.

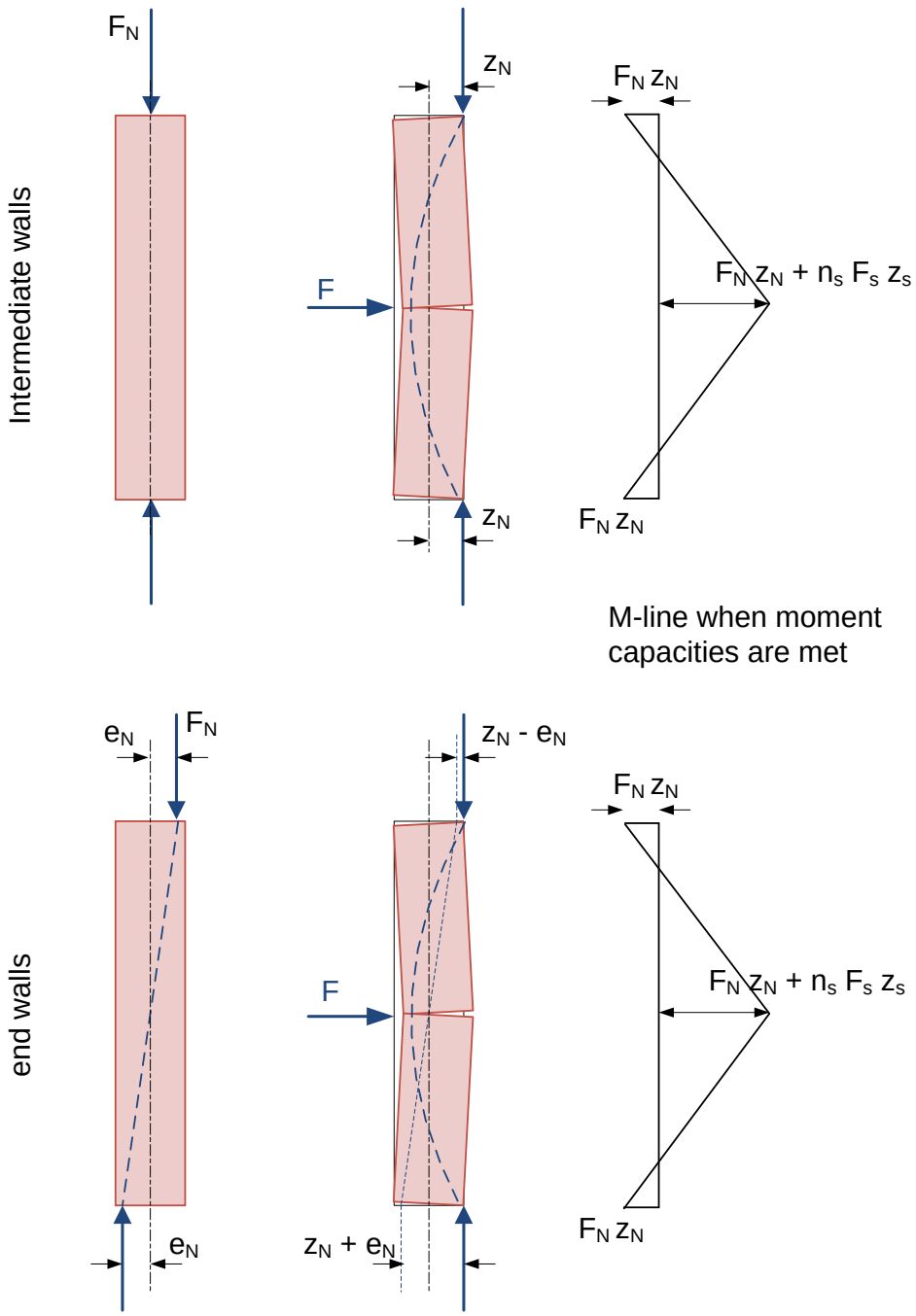

figure 39 Moment line in intermediate walls and end walls when moment capacity is met

The sum of the internal moment can be expressed as a function of δ:

$$\Sigma M_{int}(\delta) = 2F_N\, z_N(\delta) + n_s\, F_s(\delta) \left(d_s - \frac{x_u}{2} \right)$$

The sum of the external moment is influenced by the deformation of the wall. The deformation δ causes a second order effect due to the axial load:

$\Sigma M_{ext}(\delta) = ½ F l_1 + F_N \delta$

The sum of the internal moments and the sum of the external moments should be in equilibrium. From that the relation between the horizontal displacement δ and the horizontal load F can be determined.

As an example this is done for two displacements δ:

assume $\delta = 50$ mm

then

$$\Delta_s = \frac{\delta}{l_1}(d_s - x_u) = \frac{50}{1250}(50 - 18{,}9) = 1{,}25 \text{ mm}$$

$q_s = 15 \cdot 1{,}25 = 18{,}7$ N/mm

$F_s = q_s\, l_{em} = 18{,}7 \cdot 1250 = 23{,}3 \cdot 10^3$ N

$z_s = d_s - 1/2\, x_u = 50 - ½\, 18{,}9 = 40{,}6$ mm

$z_N = (t - x_u)/2 = (100 - 18{,}9)/2 = 40{,}6$ mm

$\Sigma M_{int} = n_s F_s z_s + 2 \cdot z_N F_N = 2{,}7 \cdot 23{,}3 \cdot 10^3 \cdot 40{,}6 + 2 \cdot 40{,}6 \cdot 18 \cdot 10^3 = 4{,}02 \cdot 10^6$ Nmm

$$F = 2\frac{\Sigma M_{int} - F_N \delta}{l_1} = 2\frac{4{,}02 \cdot 10^6 - 18 \cdot 10^3 \cdot 50}{1250} = 5{,}0 \cdot 10^3 \text{ N}$$

assume $\delta = 120$ mm

then

$$\Delta_s = \frac{\delta}{l_1}(d_s - x_u) = \frac{120}{1250}(50 - 18{,}9) = 3{,}0 \text{ mm}$$

$q_s = 45$ N/mm

$F_s = q_s\, l_{em} = 45 \cdot 1250 = 56{,}2 \cdot 10^3$ N

$z_s = 40{,}6$ mm

$z_N = 40{,}6$ mm

$\Sigma M_{int} = n_s F_s z_s + 2 \cdot z_N F_N = 2{,}7 \cdot 56{,}2 \cdot 10^3 \cdot 40{,}6 + 2 \cdot 40{,}6 \cdot 18 \cdot 10^3 = 7{,}62 \cdot 10^6$ Nmm

$$F = 2\frac{\Sigma M_{int} - F_N \delta}{l_1} = 2\frac{7{,}62 \cdot 10^6 - 18 \cdot 10^3 \cdot 120}{1250} = 8{,}7 \cdot 10^3 \text{ N}$$

The complete result of the push-over calculation is presented in figure 40.

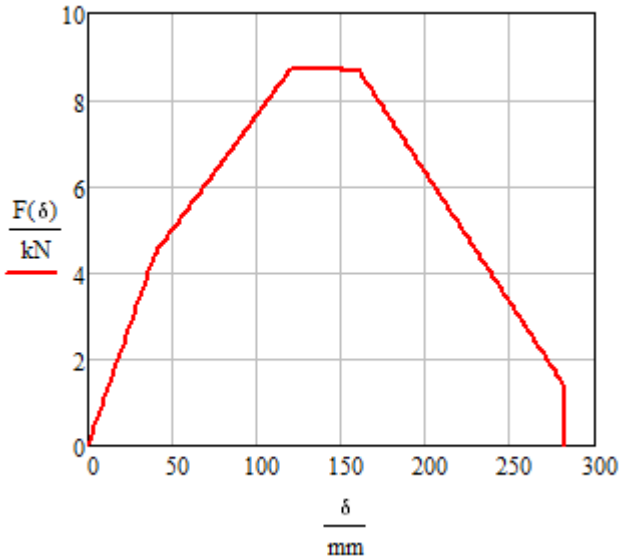

figure 40 Result of push-over calculation

Determination of the natural period and the behaviour factor
First the result of the push-over calculation is transformed to a bilinear behaviour. This is done according figure 3.1 of *Frumento, S e.o. Interpretation of experimental shear tests on clay brick masonry walls and evaluation of q-factors for seismic design. IUSS Press, 2009.* see figure 41. This approach is consistent with the approach in NEN-EN 1998-3 where in annex C the ultimate displacement capacity is defined as the displacement where the resistance is dropped back to 80% of the maximum capacity.

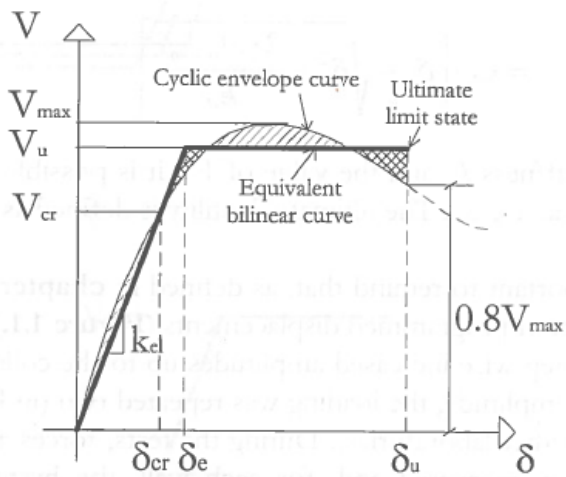

figure 41 Transformation of result push-over behaviour according Frumento [2009]

First the stiffness of the first linear behaviour is determined. This is done at the point where the slip Δ_s equals just 1 mm. In that case the displacement δ follows from:

$$\delta = \Delta_s \frac{l_1}{d_s - x_u} = 40 \text{ mm}$$

At this displacement the horizontal force F equals 4,47 kN. So the value for the stiffness k_e follows form:

$$k_e = \frac{F}{\delta} = \frac{4470}{40} = 111 \text{ N/mm}$$

The maximum value of F, F_m, equals 8,73 kN and appears at a displacement of 120 mm. From this it is chosen to end the considered behaviour at a load of 80% of the maximum: 0,8·8,73 = 6,98 kN. This load is found at a displacement δ_u equal of 189 mm.

The total energy below the curve of the nonlinear push-over behaviour is found from:

$$E = \int_0^{\delta_u} F(x)\,dx = 1190 \cdot 10^3 \text{ Nmm}$$

From this the maximum force in the bilinear relation can be found:

$$F_{Rm} = k_e \left[\delta_u - \sqrt{\frac{k_e \delta_u^2 - 2E}{k_e}} \right] = 111 \left[189 - \sqrt{\frac{111 \cdot 189^2 - 2 \cdot 1190 \cdot 10^3}{111}} \right] = 7{,}7 \cdot 10^3 \text{ N}$$

$$\delta_e = \frac{F_{Rm}}{k_e} = \frac{7700}{111} = 69{,}3 \text{ mm}$$

The resulting bilinear push-over relation is presented in figure 42.

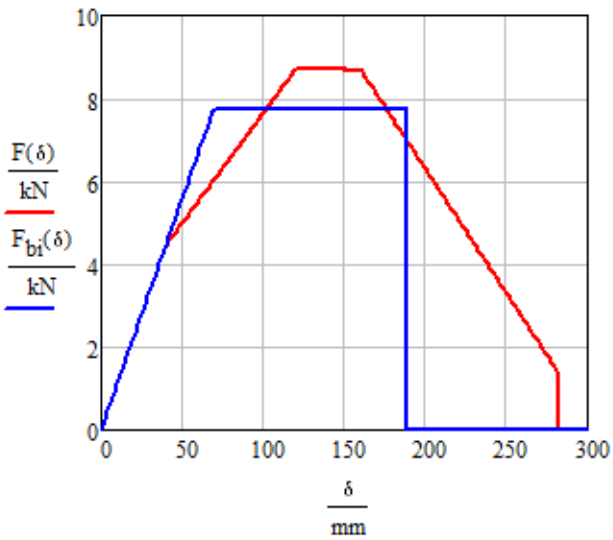

figure 42 Graphical presentation of bilinear push-over relation in blue line

From this relation the natural period and the behaviour factor can be found. When a beam with a constant mass is schemed as a beam with a concentrated mass, the equivalent mass equals half the total mass of the beam:

mass: 0,5 b t l γ = 0,5·1·0,1·2,5·1800 = 225 kg

The natural period follows from:

$$T_1 = 2\pi\sqrt{\frac{mass}{k_e}} = 2\pi\sqrt{\frac{225}{111\cdot 10^3}} = 0{,}283 \text{ s}$$

$$\mu = \frac{\delta_u}{\delta_e} = \frac{189}{69{,}3} = 2{,}72$$

$$q = \sqrt{2\mu - 1} = \sqrt{2\cdot 2{,}72 - 1} = 2{,}11$$

Conform 3.2.2.2.3 of the NPR 9998 this value of q may be multiplied with a factor 1,33, so

q = 1,33q = 2,81

Determination of the static equivalent load
For the value of the behaviour factor q and the given peak ground accelaration the design spectrum can be made according NPR 9998, see figure 43.

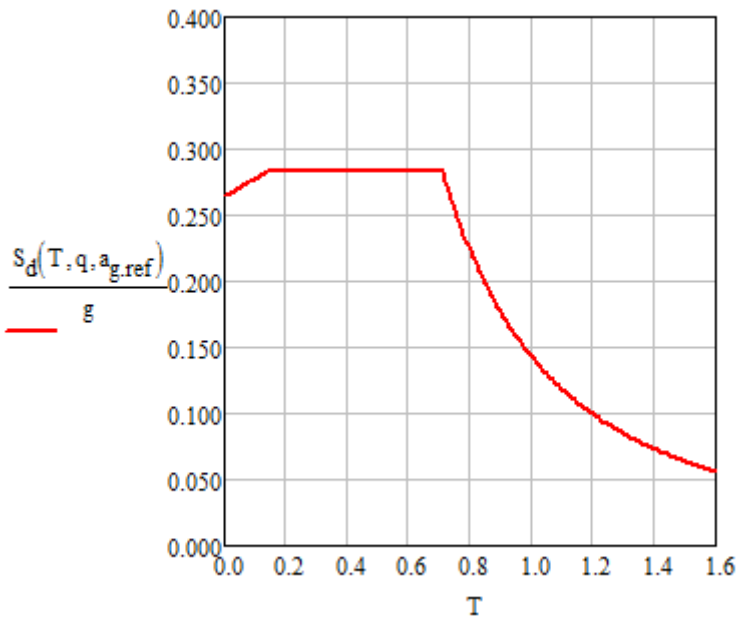

figure 43 Design spectrum for q = 2,81 and $a_{g,ref}$ = 0,2 g

From this the value for S_d equals 0,283 g.

The static equivalent load equals:
$p_{Ed} = b\ t\ \gamma\ S_d = 1\cdot 0{,}1\cdot 1800\cdot 0{,}283\cdot 10 = 509$ N/m

Capacity check
The check of the capacity will be based on clause 4.4.2.2 of NPR 9998.
The sum of the internal moments follows from:

$$\Sigma M_{Ed} = \frac{1}{8} p_{Ed}\, l^2 + F_N\, \delta_N = \frac{1}{8} 0{,}509 \cdot 2{,}5^2 + 18 \cdot 0{,}189 = 3{,}79 \text{ kNm}$$

The design value of the moment resistance follows from:
$\gamma_m = 1{,}5$

The moment resistance is also determined for the situation where the ultimate displacement is present: $\delta_u = 189$ mm

$$\Delta_s = \frac{\delta}{l_1} (d_s - x_u) = \frac{189}{1250} (50 - 18{,}9) = 4{,}7 \text{ mm}$$

$q_s = 50 - 5{,}7(4{,}7 - 4 \text{ mm}) = 46$ N/mm
$F_s = q_s\, l_{em} = 46 \cdot 1250 = 57{,}5 \cdot 10^3$ N

$z_s = 40{,}6$ mm
$z_N = 40{,}6$ mm

$$\Sigma M_{int} = n_s\, F_s\, z_s + 2 \cdot z_N F_N = 2{,}7 \cdot 57{,}5 \cdot 10^3 \cdot 40{,}6 + 2 \cdot 40{,}6 \cdot 18 \cdot 10^3 = 7{,}76 \cdot 10^6 \text{ Nmm}$$

The design value of the sum of the moment resistance follows from:

$$\Sigma M_{Rd} = \frac{0{,}81 \Sigma M_{int}}{\gamma_m \gamma_M} = \frac{0{,}81 \cdot 7{,}76}{1{,}5 \cdot 1{,}1} = 3{,}81 \text{ kNm}$$

It is concluded that the design value of the sum moments due to the effect of the load ΣM_{Ed} is smaller that the design value of the sum of the moment resistance ΣM_{Rd}. The ratio equals:

$$\frac{\Sigma M_{Ed}}{\Sigma M_{Rd}} = \frac{3{,}79}{3{,}81} = 0{,}99$$

The structure full fills the requirements.

4.3 Example calculation B

Hereafter an example of the same load bearing wall as considered in example calculation A is presented. However in this calculation the deformation capacity is limited more so the influence of the second order effect will be limited. Therefore, the results of the calculation are identical until the determination of the nonlinear push-over behaviour as described in figure 40.
From there on it is assumed that the ultimate displacement δ_u equals 100 mm,

Determination of the natural period and the behaviour factor
The total energy below the curve of the nonlinear push-over behaviour is found from:

$$E = \int_0^{\delta_u} F(x)\, dx = 452 \cdot 10^3 \text{ Nmm}$$

From this the maximum force in the bilinear relation can be found:

$$F_{Rm} = k_e \left[\delta_u - \sqrt{\frac{k_e \delta_u^2 - 2E}{k_e}} \right] = 111 \left[100 - \sqrt{\frac{111 \cdot 100^2 - 2 \cdot 452 \cdot 10^3}{111}} \right] = 6{,}3 \cdot 10^3 \text{ N}$$

$$\delta_e = \frac{F_{Rm}}{k_e} = \frac{6300}{111} = 56{,}7 \text{ mm}$$

The resulting bilinear push-over relation is presented in figure 44.

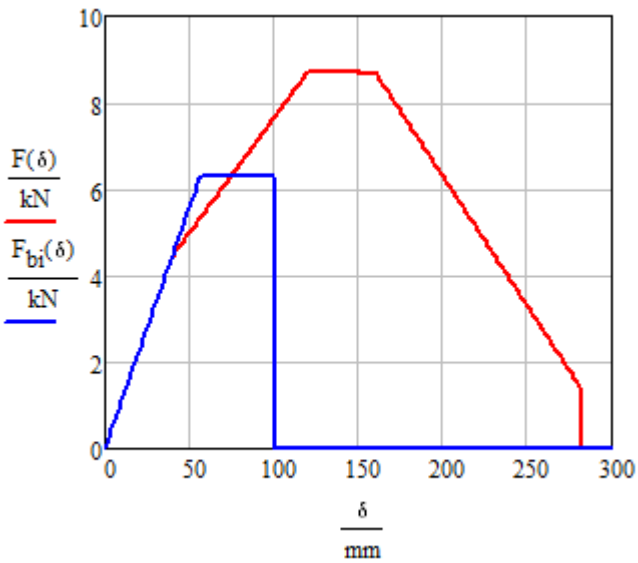

figure 44 Graphical presentation of bilinear push-over relation in blue line

From this relation the natural period and the behaviour factor can be found:

mass: $0{,}5\ b\ t\ l\ \gamma = 0{,}5 \cdot 1 \cdot 0{,}1 \cdot 2{,}5 \cdot 1800 = 225$ kg

The natural period follows from:

$$T_1 = 2\pi \sqrt{\frac{\text{mass}}{k_e}} = 2\pi \sqrt{\frac{225}{111 \cdot 10^3}} = 0{,}283 \text{ s}$$

$$\mu = \frac{\delta_u}{\delta_e} = \frac{100}{56{,}7} = 1{,}76$$

$$q = \sqrt{2\mu - 1} = \sqrt{2 \cdot 1{,}76 - 1} = 1{,}59$$

Conform 3.2.2.2.3 of the NPR 9998 this value of q may be multiplied with a factor 1,33, so

$q = 1{,}33q = 2{,}11$

Determination of the static equivalent load
For the value of the behaviour factor q and the given peak ground acceleration the design spectrum can be made according NPR 9998, see figure 45.

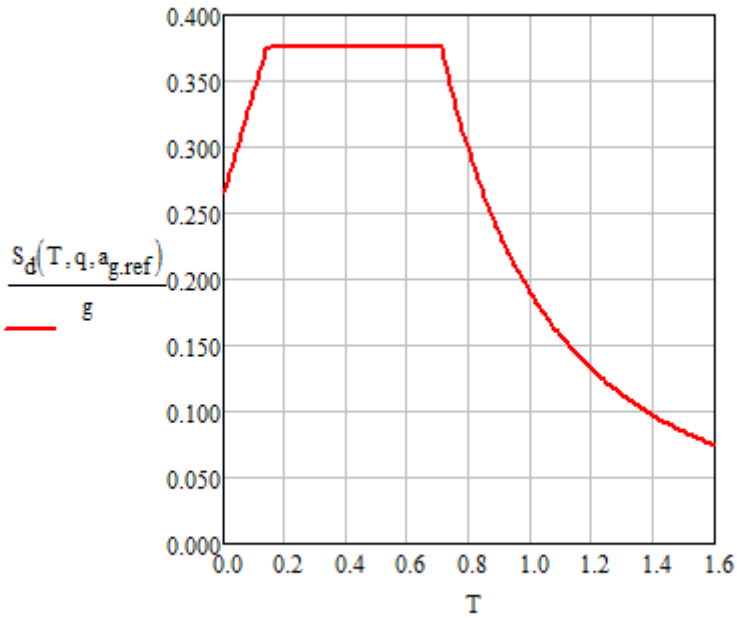

figure 45 Design spectrum for q = 2,11 and $a_{g,ref}$ = 0,2 g

From this the value for S_d equals 0,375 g.

The static equivalent load equals:
$p_{Ed} = b\ t\ \gamma\ S_d = 1 \cdot 0{,}1 \cdot 1800 \cdot 0{,}375 \cdot 10 = 663$ N/m

Capacity check
The check of the capacity will be based on clause 4.4.2.2 of NPR 9998.

The sum of the internal moments follows from:

$$\Sigma M_{Ed} = \frac{1}{8} p_{Ed}\, l^2 + F_N\, \delta_N = \frac{1}{8} 0{,}633 \cdot 2{,}5^2 + 18 \cdot 0{,}100 = 2{,}32 \text{ kNm}$$

The design value of the moment resistance follows from:
$\gamma_m = 1{,}5$

The moment resistance is also determined for the situation where the ultimate displacement is present: $\delta_u = 100$ mm

$$\Delta_s = \frac{\delta}{l_1}(d_s - x_u) = \frac{100}{1250}(50 - 18{,}9) = 2{,}5 \text{ mm}$$

$q_s = 15\Delta_s = 37{,}4$ N/mm
$F_s = q_s\, l_{em} = 37{,}4 \cdot 1250 = 46{,}7 \cdot 10^3$ N
$z_s = 40{,}6$ mm

$z_N = 40{,}6$ mm

$\Sigma M_{int} = n_s\ F_s\ z_s + 2 \cdot z_N F_N = 2{,}7 \cdot 46{,}7 \cdot 10^3 \cdot 40{,}6 + 2 \cdot 40{,}6 \cdot 18 \cdot 10^3 = 7{,}81 \cdot 10^6$ Nmm

The design value of the sum of the moment resistance follows from:

$$\Sigma M_{Rd} = \frac{0{,}81 \Sigma M_{int}}{\gamma_m \gamma_M} = \frac{0{,}81 \cdot 7{,}81}{1{,}5 \cdot 1{,}1} = 3{,}84 \text{ kNm}$$

It is concluded that the design value of the sum moments due to the effect of the load ΣM_{Ed} is smaller than the design value of the sum of the moment resistance ΣM_{Rd}. The ratio equals:

$$\frac{\Sigma M_{Ed}}{\Sigma M_{Rd}} = \frac{2{,}32}{3{,}84} = 0{,}60$$

The structure full fills the requirements. Also it can be learned that for load bearing walls the limitation of the ultimate capacity will lead to a more economically design.

4.4 Example calculation C

4.4.1 General

Hereafter another example of a load bearing wall is presented. The calculation is performed as a calculation in which a chosen design is checked. The calculation is performed for a QSC type wall.

Input for the calculation

height of the wall	$l = 2500$ mm
width of the wall	$b = 1000$ mm
thickness of the masonry wall	$t_m = 100$ mm
thickness of the cement-matrix	$t_c = 15$ mm
number of strips per width	$n_s = 1{,}5$
effective depth of the strips	$d_s = 50$ mm
axial load on the wall	$F_N = 8$ kN
unit mass of masonry	$\gamma = 1800$ kg/m³
mean compressive strength masonry	$f_m = 7{,}0$ N/mm²
unit mass of reinforced cement-matrix	$\gamma = 2400$ kg/m³
tensile strength	$f_{ct} = 5$ MPa
ultimate strain	$\varepsilon_{ctu} = 0{,}016$
peak ground acceleration	$a_{g,ref} = 0{,}25$ g
factor for design value pga	$k_{ag} = 1{,}4$
partial factor for resistance	$\gamma_M = 1{,}1$

4.4.2 Modelling different behaviour QSC wall

When the behaviour of the QSC wall in the direction where the reinforced cement-matrix is under tension is modelled based on the tensile capacity of this material (first peak), its stiffness is much larger than when the capacity is based on the polymer strips. The force-displacement behaviour of the wall is like presented in figure 46.

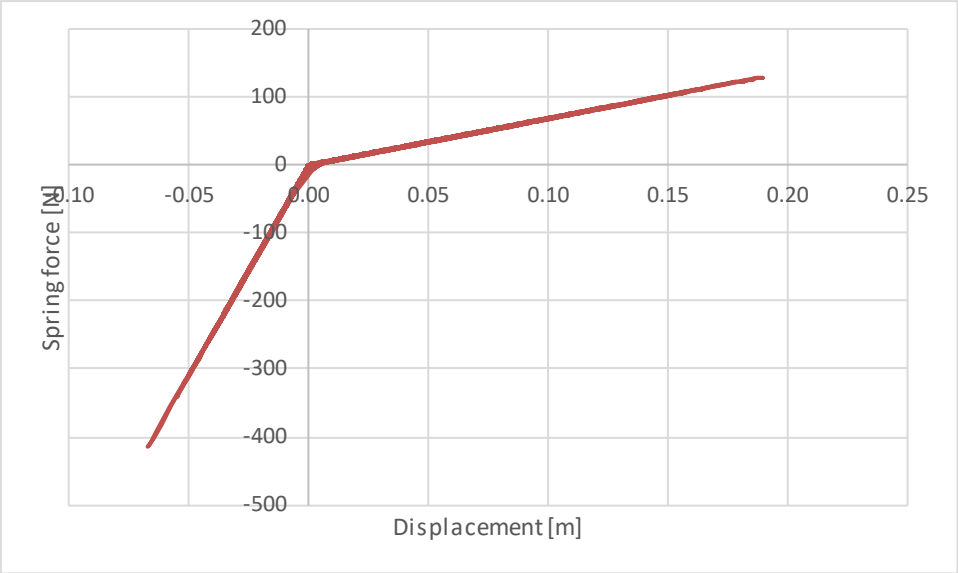

figure 46 Force-displacement relation for a QSC wall

Due that the behaviour is not linear and equal in both directions it cannot be described by one linear calculation. In annex A, from an example non-linear time-history calculation it is shown that the behaviour of the wall can be checked by performing two linear calculations. One based on the stiff properties (QSC+ first peak) and one based on the less stiff properties (QSC-).

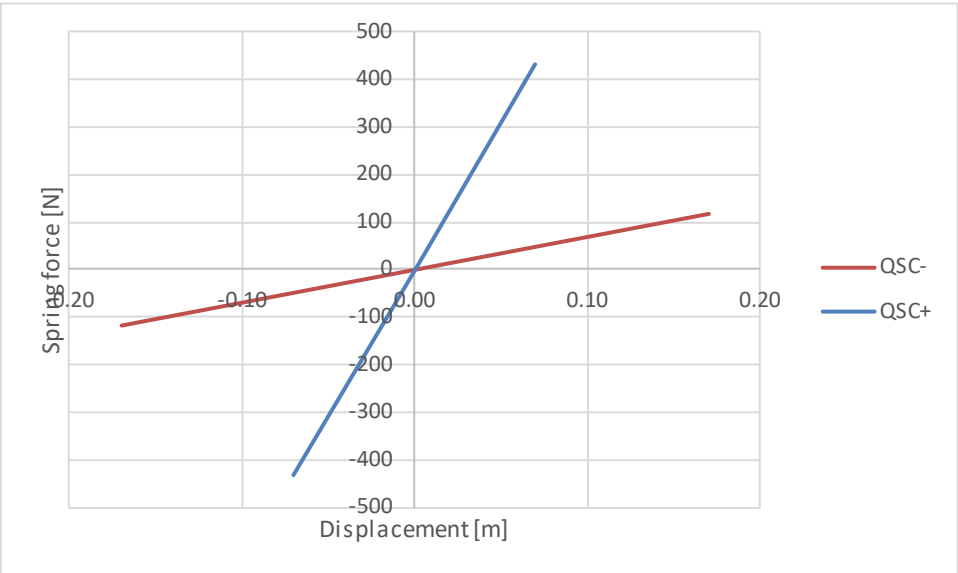

figure 47 Force-displacement relation for a QSC+ wall and the QSC- wall

Hereafter an example of a load bearing wall is presented. The calculation is performed as a calculation in which a chosen design is checked. The calculation is performed for a QSS type wall.

4.4.3 Checking QSC+ (stiff)

Hereafter a linear behaviour of the wall is assumed.

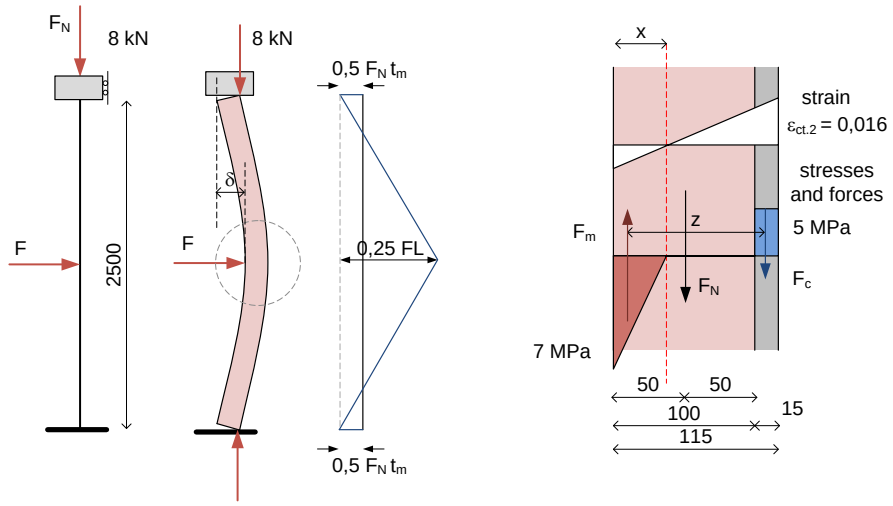

figure 48 Model for structural behaviour of specimen in a three point bending test

The properties of the reinforced cement-matrix are summarized hereafter:
f_{ct} = 5 MPa
$\varepsilon_{ct.u}$ = 0,016

The maximum tensile force in the reinforced cement-matrix follows from:
$F_{ct} = b\ t_c\ f_{ct} = 1000 \cdot 15 \cdot 5 = 75 \cdot 10^3$ N

The depth of the compression zone in the masonry can be approximated by:
$x = 2(F_{ct} + F_N)/(b\ f_m) = 2(75 + 8)/(7) = 23{,}7$ mm

The moment resistance results from:
$z_c = t_m - x/3 + t_c/2 = 100 - 23{,}7/3 + 15/2 = 99{,}6$ mm
$z_N = t_m/2 - x/3 = 100/2 - 23{,}7/2 = 38{,}1$ mm
$M_R = F_{ct}\ z_c + F_N\ z_N = 75 \cdot 0{,}0996 + 8 \cdot 0{,}0381 = 7{,}47 + 0{,}30 = 7{,}77$ kNm

The ultimate curvature can be calculated from:
$\kappa_R = \varepsilon_{ct.u}/(t_t - x) = 0{,}016/(0{,}115 - 0{,}0237) = 0{,}175\ m^{-1}$

Based on the ultimate moment resistance the maximum horizontal load on the specimen follows from the following equation:

$$F = \frac{4}{L}\left(M_R + F_N \frac{t_m}{2}\right) = \frac{4}{2{,}5}\left(7{,}77 + 8\frac{0{,}1}{2}\right) = 13{,}0 \text{ kN}$$

Based on the distribution of the moment at extreme loading and the known curvature the maximum displacement can be estimated as:

$$L_m = L\frac{M_R}{M_R + F_N\frac{t_m}{2}} = 2{,}5\frac{7{,}77}{7{,}77 + 8\frac{0{,}1}{2}} = 2{,}38$$

$\delta = \kappa_R\ L\ L_m/15 = 0{,}175 \cdot 2{,}5 \cdot 2{,}38/15 = 0{,}069$ m

A linear relation between the force and displacement is assumed. The stiffness of the system follows from:

$k_e = F/\delta = 13 \cdot 10^3/0{,}069 = 188 \cdot 10^3$ N/m

From this relation the natural period and the behaviour factor can be found:

mass per unit: $p_{mas} = t_m\ \gamma_{mas} + t_c\ \gamma_{cem} = 0{,}1 \cdot 1800 + 0{,}015 \cdot 2400 = 216$ kg/m²

mass = $0{,}5\ b\ \ l\ p_{mas} = 0{,}5 \cdot 1 \cdot 2{,}5 \cdot 216 = 270$ kg

The natural period follows from:

$$T_1 = 2\pi\sqrt{\frac{\text{mass}}{k_e}} = 2\pi\sqrt{\frac{277}{188 \cdot 10^3}} = 0{,}24 \text{ s}$$

The behaviour factor is depending on the ductility of the system. The ductility of this system is limited due to the fact that the resistance is based on the tensile strength of the reinforced cement-matrix, for which no softening behaviour is considered, so:

$q = 1$

Determination of the static equivalent load
For the value of the behaviour factor q and the given peak ground acceleration the design spectrum can be made according NPR 9998 (dec 2015). For a peak ground acceleration of 0,25 g, $k_{ag} = 1{,}4$, T = 0,24 s and q = 1, the following value for S_d results:

$S_d = 0{,}91$ g.

The static equivalent load equals:
$p_{Ed} = b\ p_{mas}\ S_d = 1 \cdot 277 \cdot 0{,}91 \cdot 10 = 2520$ N/m

Capacity check
The check of the capacity will be based on clause 4.4.2.2 of NPR 9998.

The moment at the top and the foot of the wall equals:
$M_{top} = F_N\ t_m/2 = 8 \cdot 0{,}05 = 0{,}40$ kNm

The moment at midspan can be derived from
$M_m = \frac{1}{8}\ p_{Ed}\ l^2 - M_{top} = \frac{1}{8}\ 2{,}52 \cdot 2{,}5^2 - 0{,}40 = 1{,}57$ kNm

The design value of the moment resistance follows from:

$$M_d = \frac{M_R}{\gamma_m \gamma_M} = \frac{7,77}{1,5 \cdot 1,1} = 4,71 \text{ kNm}$$

The capacity of the wall when the reinforced cement-matrix is tensioned, is sufficient to withstand the earthquake effect.

4.4.4 Checking QSC- (less stiff)

The calculation for QSC- is conducted in the same way the calculations for a QSS-type wall are made. The difference is that it can be assumed that the compression force can be resisted by the cement-matrix, so the depth of the compression zone is effectively reduced, and that the effective depth of the CFRP-strips is increased with 15 mm.

Nonlinear push-over calculation
$l_1 = l/2 = 1250$ mm
$l_{em} = l_1 = 1250$ mm

$t_t = 115$ mm
$d_s = 65$ mm
$f_m = 20,0$ N/mm² (assumption for the mean compressive strength of the CEM-layer)

$F_{s.max} = l_{em}\, q_{s,max} = 1250 \cdot 50 = 62,5 \cdot 10^3$ N

$$x_u = \frac{F_N + n_s F_{s,max}}{b\, f_m} = \frac{8 \cdot 10^3 + 1,5 \cdot 62,5 \cdot 10^3}{1000 \cdot 20,0} = 5,1 \text{ mm}$$

The rotation φ can be expressed as a function of the displacement δ:

$$\varphi(\delta) = \frac{\delta}{l_1}$$

From this also the slip of the strip Δ_s can be expressed as a function of δ:

$$\Delta_s(\delta) = \varphi(\delta)\,(d_s - x_u)$$

From Δ_s the value for the bond force q_s can be derived from the following relation:

$q_s = 15\,\Delta_s$	when $\Delta_s \leq 3$ mm
$q_s = 45 + 5(\Delta_s - 3 \text{ mm})$	when $3 \text{ mm} < \Delta_s \leq 4$ mm
$q_s = 50 - 5,7(\Delta_s - 4 \text{ mm})$	when $4 \text{ mm} < \Delta_s \leq 7$ mm
$q_s = 0$	when $7 \text{ mm} < \Delta_s$

and therefor can be expressed as a function of δ.

From the embedded length l_{em} and q_s the force in one strip can be found:

$F_s(\delta) = q_s(\delta)\, l_{em}$

The force in the strip should be limited to its capacity. For the standard strips 20×1,4 mm² this equals 78,5 kN. This capacity will be reached when the embedded length equals 1,57 m. In this case the embedded length is smaller so failure of the strip is not expected.

The internal lever arm of the axial force, z_N, which is active both at the connection with the floors and at midspan, is depending on Δ_s and therefor depending on the displacement δ:

$$z_N(\delta) = \frac{t - x_u}{2} \frac{\Delta_s(\delta)}{1\,\text{mm}} \qquad \text{when } \Delta_s(\delta) \le 1 \text{ mm}$$

$$z_N(\delta) = \frac{t - x_u}{2} \qquad \text{when } \Delta_s(\delta) > 1 \text{ mm}$$

For the wall considered the sum of the internal moment capacity is determined. Due to the expected great displacements, it is assumed that for both intermediate walls and for end walls the moment capacity at the end of the wall equals $F_N\, z_N$ at both ends, see figure 39.

The sum of the internal moment can be expressed as a function of δ:

$$\Sigma M_{int}(\delta) = 2F_N\, z_N(\delta) + n_s\, F_s(\delta) \left(d_s - \frac{x_u}{2} \right)$$

The sum of the external moment is influenced by the deformation of the wall. The deformation δ causes a second order effect due to the axial load:

$\Sigma M_{ext}(\delta) = ½\, F\, l_1 + F_N\, \delta$

The sum of the internal moments and the sum of the external moments should be in equilibrium. From that the relation between the horizontal displacement δ and the horizontal load F can be determined.

As an example this is done for a displacements δ = 50 mm:

$$\Delta_s = \frac{\delta}{l_1}(d_s - x_u) = \frac{50}{1250}(65 - 5{,}1) = 2{,}40 \text{ mm}$$

$q_s = 15 \cdot 2{,}40 = 36{,}0$ N/mm

$F_s = q_s\, l_{em} = 36{,}0 \cdot 1250 = 44{,}9 \cdot 10^3$ N

$z_s = d_s - 1/2\, x_u = 65 - ½\, 5{,}1 = 62{,}4$ mm

$z_N = (t - x_u)/2 = (115 - 5{,}1)/2 = 54{,}9$ mm

$\Sigma M_{int} = n_s\, F_s\, z_s + 2 \cdot z_N F_N = 1{,}5 \cdot 44{,}9 \cdot 10^3 \cdot 62{,}4 + 2 \cdot 54{,}9 \cdot 8 \cdot 10^3 = 5{,}09 \cdot 10^6$ Nmm

$$F = 2\frac{\Sigma M_{int} - F_N\delta}{l_1} = 2\frac{5{,}09\cdot 10^6 - 8\cdot 10^3\cdot 50}{1250} = 7{,}50\cdot 10^3\ \text{N}$$

The complete result of the push-over calculation is presented in figure 49.

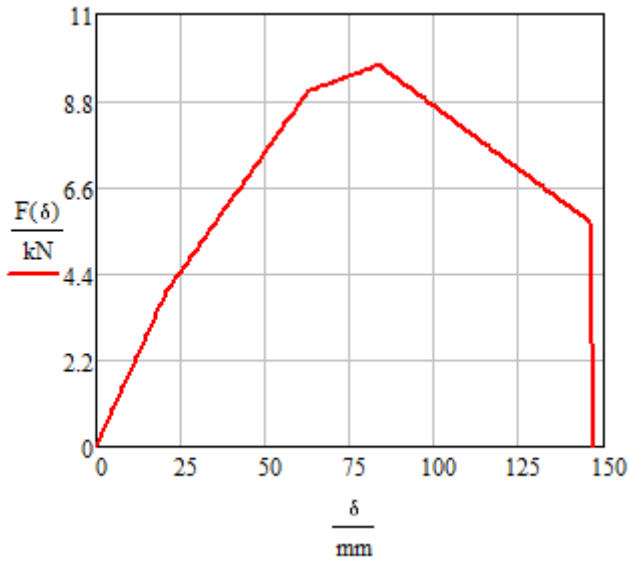

figure 49 Result of push-over calculation

Determination of the natural period and the behaviour factor
First the result of the push-over calculation is transformed to a bilinear behaviour. This is done according figure 3.1 of *Frumento, S e.o. Interpretation of experimental shear tests on clay brick masonry walls and evaluation of q-factors for seismic design. IUSS Press, 2009.* see figure 41. This approach is consistent with the approach in NEN-EN 1998-3 where in annex C the ultimate displacement capacity is defined as the displacement where the resistance is dropped back to 80% of the maximum capacity.

First the stiffness of the first linear behaviour is determined. This is done at the point where the slip Δ_s equals just 1 mm. In that case the displacement δ follows from:

$$\delta = \Delta_s\frac{l_1}{d_s - x_u} = 21\ \text{mm}$$

At this displacement the horizontal force F equals 3,95 kN. So the value for the stiffness k_e follows from:

$$k_e = \frac{F}{\delta} = \frac{3950}{21} = 189\ \text{N/mm}$$

The maximum value of F, F_m, equals 9,69 kN and appears at a displacement of 83 mm. From this it is chosen to end the considered behaviour at a load of 80% of the maximum: 0,8·9,69 = 7,75 kN. This load is found at a displacement δ_u equal of 114 mm.

The total energy below the curve of the nonlinear push-over behaviour is found from:

$$E = \int_0^{\delta_u} F(x)\,dx = 774 \cdot 10^3 \text{ Nmm}$$

From this the maximum force in the bilinear relation can be found:

$$F_{Rm} = k_e \left[\delta_u - \sqrt{\frac{k_e \delta_u^2 - 2E}{k_e}} \right] = 189 \left[114 - \sqrt{\frac{189 \cdot 114^2 - 2 \cdot 774 \cdot 10^3}{189}} \right] = 8{,}4 \cdot 10^3 \text{ N}$$

$$\delta_e = \frac{F_{Rm}}{k_e} = \frac{8400}{189} = 44{,}6 \text{ mm}$$

The resulting bilinear push-over relation is presented in figure 50.

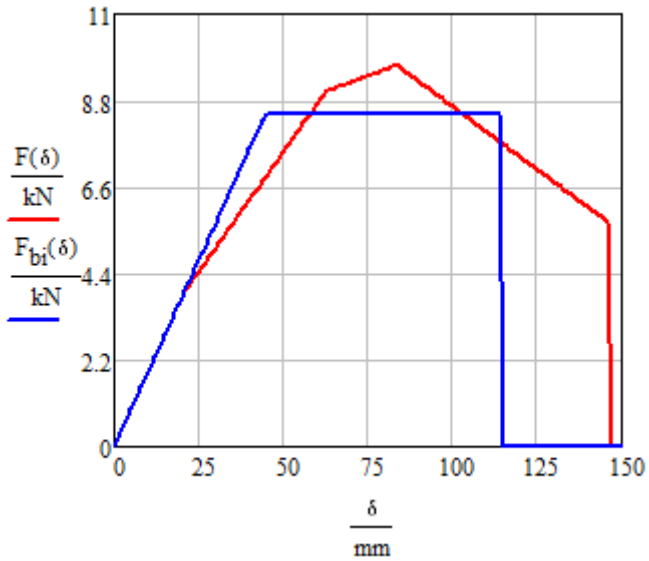

figure 50 Graphical presentation of bilinear push-over relation in blue line

From this relation the natural period and the behaviour factor can be found. When a beam with a constant mass is schemed as a beam with a concentrated mass, the equivalent mass equals half the total mass of the beam:

mass: $0{,}5\ b\ t\ l\ \gamma = 0{,}5 \cdot 1 \cdot 0{,}115 \cdot 2{,}5 \cdot 1800 = 259$ kg

The natural period follows from:

$$T_1 = 2\pi \sqrt{\frac{\text{mass}}{k_e}} = 2\pi \sqrt{\frac{259}{189 \cdot 10^3}} = 0{,}232 \text{ s}$$

$$\mu = \frac{\delta_u}{\delta_e} = \frac{114}{44{,}6} = 2{,}56$$

$$q = \sqrt{2\mu - 1} = \sqrt{2 \cdot 2{,}56 - 1} = 2{,}03$$

The ductility of the wall loaded in this direction is considered to be relatively high. So, conform 3.2.2.2.3 of the NPR 9998, this value of q may be multiplied with a factor 1,33:

q = 1,33q = 2,70

Determination of the static equivalent load
For the value of the behaviour factor q and the given peak ground accelaration the design spectrum can be made according NPR 9998, see figure 51.

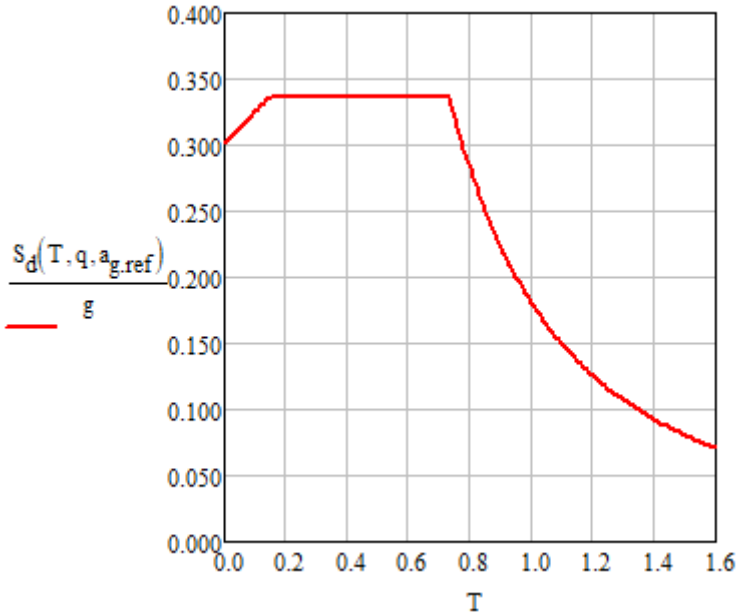

figure 51 Design spectrum for q = 2,70 and $a_{g,ref}$ = 0,25 g

From this the value for S_d equals 0,336 g.

The static equivalent load equals:
$p_{Ed} = b\ t\ \gamma\ S_d = 1 \cdot 0{,}115 \cdot 1800 \cdot 0{,}336 \cdot 10 = 682$ N/m

Capacity check
The check of the capacity will be based on clause 4.4.2.2 of NPR 9998.
The sum of the internal moments follows from:

$$\Sigma M_{Ed} = \frac{1}{8} p_{Ed}\, l^2 + F_N\, \delta_N = \frac{1}{8} 0{,}682 \cdot 2{,}5^2 + 8 \cdot 0{,}114 = 1{,}44 \text{ kNm}$$

The design value of the moment resistance follows from:
$\gamma_m = 1{,}5$

The moment resistance is also determined for the situation where the ultimate displacement is present: δ_u = 123 mm. The design value of the sum of the moment resistance follows from:

$$\Sigma M_{Rd} = \frac{0{,}81\Sigma M_{int}}{\gamma_m \gamma_M} = \frac{0{,}81 \cdot 5{,}76}{1{,}5 \cdot 1{,}1} = 2{,}83 \text{ kNm}$$

It is concluded that the design value of the sum moments due to the effect of the load ΣM_{Ed} is smaller than the design value of the sum of the moment resistance ΣM_{Rd}. The ratio equals:

$$\frac{\Sigma M_{Ed}}{\Sigma M_{Rd}} = \frac{2{,}83}{5{,}76} = 0{,}51$$

The capacity of the wall when the polymer strips are tensioned and the CEM-layer is under compression, is sufficient to withstand the earthquake effect. The considered wall fulfils the requirements in both out of plane directions.

5 Summary

In this report different models are presented that can be used to describe the push-over relation of both non load bearing and load bearing masonry walls of which the properties are enhanced by applying the QuakeShield system. The presented models are based and verified on experimental research performed by both QuakeShield BV and the TU/e.

After this, it is described how the push-over calculations can be used for the design of both load bearing and non-load bearing masonry walls that are loaded by an out of plane load that is caused by the earthquakes that can appear in the Northeast of the Netherlands. For this three example calculations are presented. One for the basic configuration of the QuakeShield system. A second one for the same configuration where the ultimate displacement is limited to reduce the unfavourable second order effect. A third calculation is performed for a load bearing QSC wall where both the stiff and less stiff behaviour is considered.

Rijswijk, 15nd of November 2017.

Prof.ir. S.N.M. Wijte

ir. B. van den Broek

Annex A – NLTH Behaviour of Non-linear specimen

Hereafter the response of three systems to an identical accelerogram is presented:

- a nonlinear behaviour
- a linear stiff behaviour
- a linear less stiff behaviour.

Accelerogram

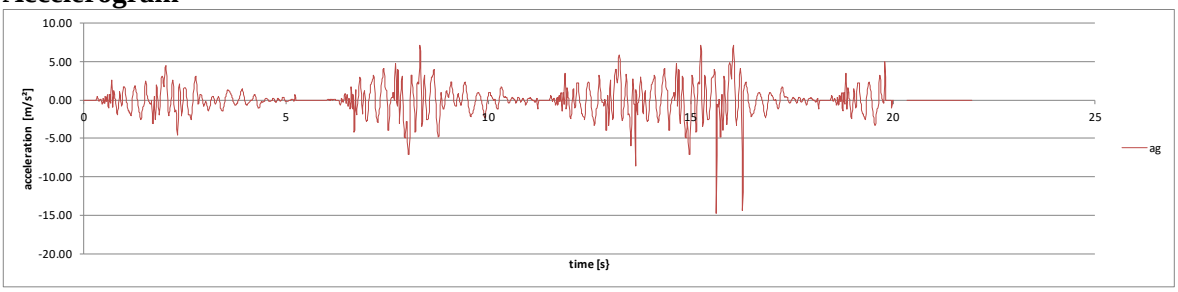

Nonlinear behaviour

mass	25 kg
spring stiffness	685 N/m
	6168 N/m
damping	5 %

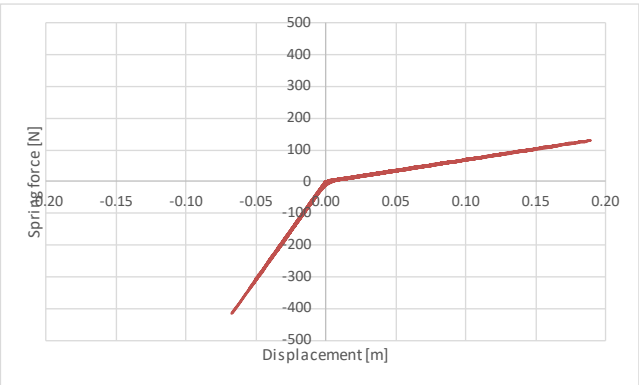

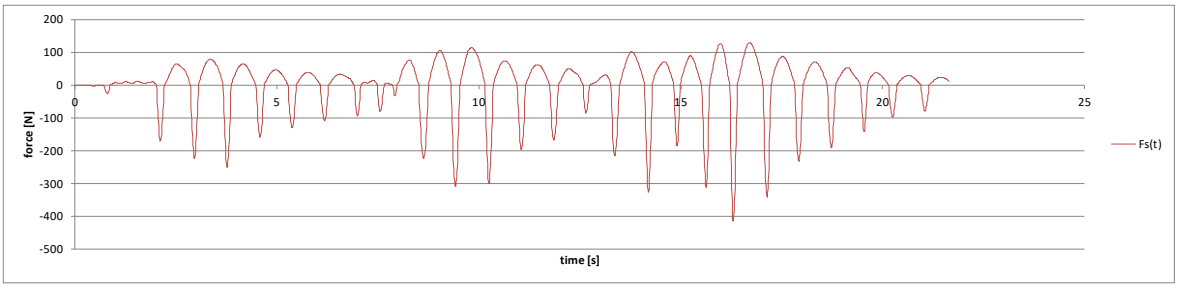

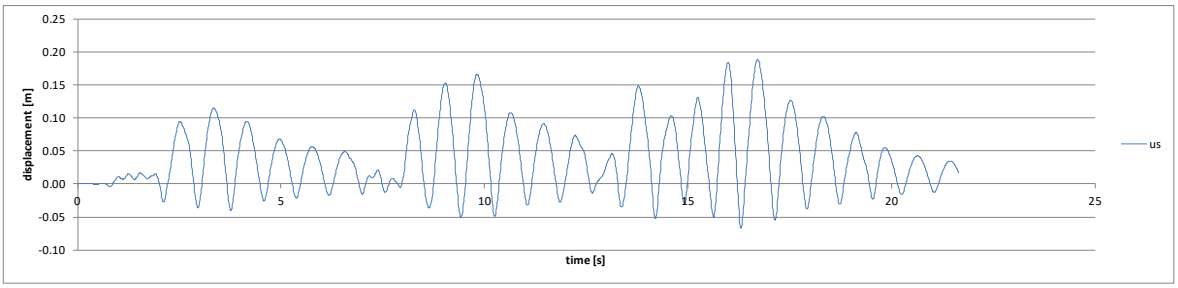

	Extreme forces:	Extreme displacement:
stiff	-413 N	-0,067 m
less stiff	129 N	0,189 m

Stiff behaviour

mass	25 kg
spring stiffness	6168 N/m
damping	5 %

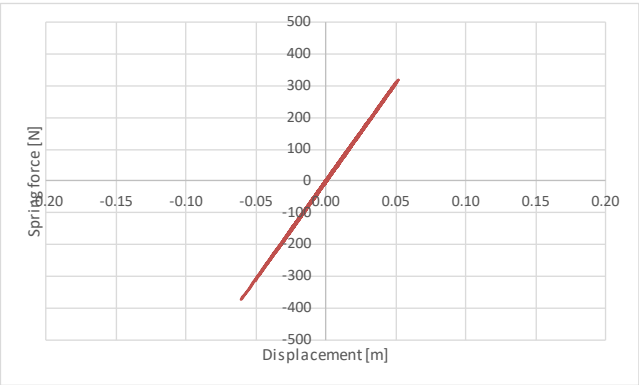

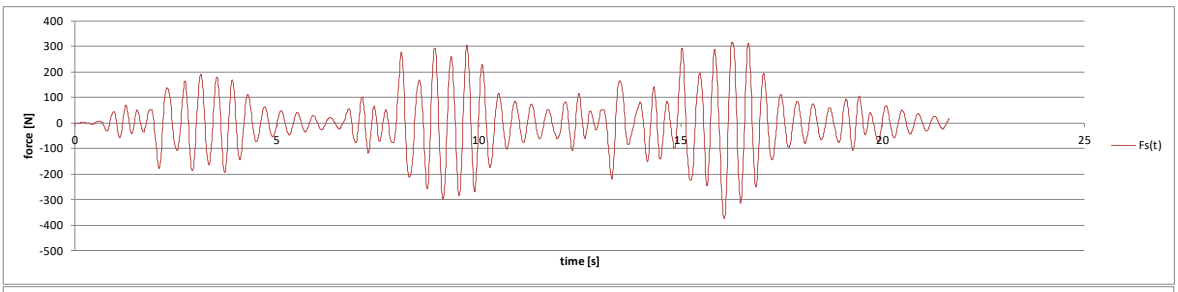

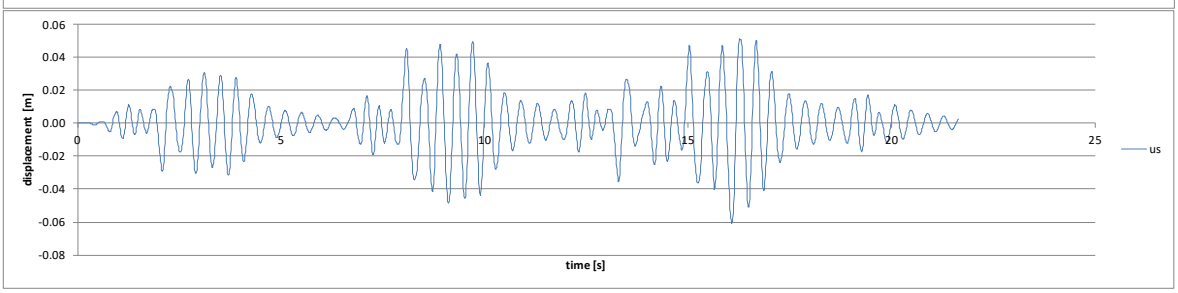

	Extreme forces:	Extreme displacement:
stiff	-376 N	-0,061 m
	315 N	0,051 m

Less stiff behaviour

mass	25 kg
spring stiffness	685 N/m
damping	5 %

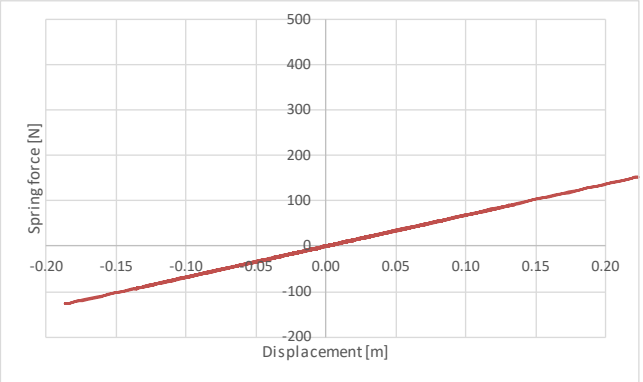

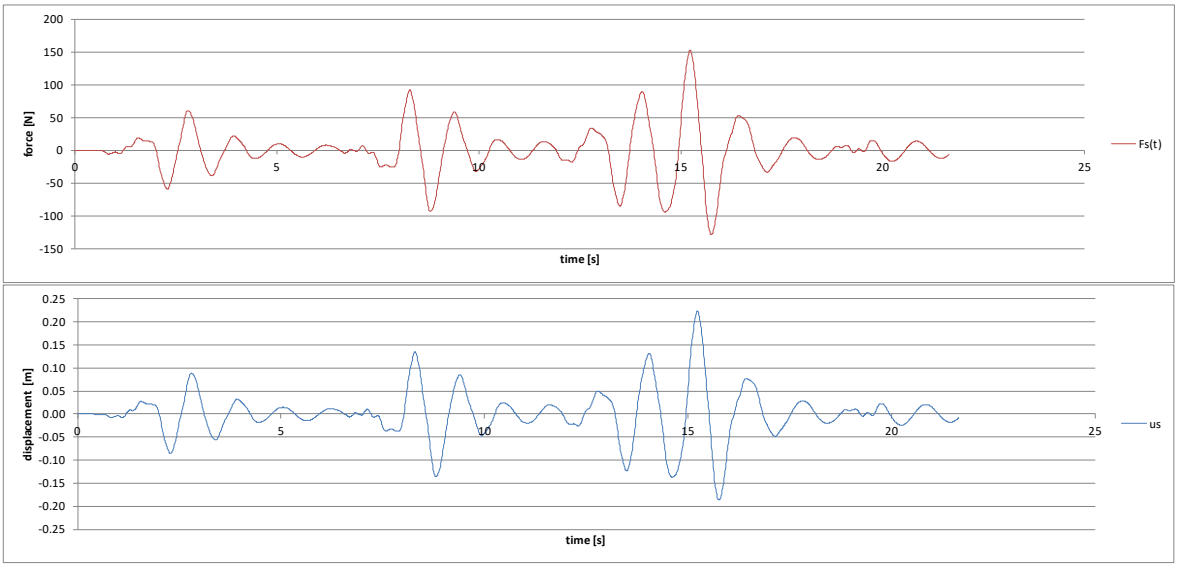

	Extreme forces:	Extreme displacement:
less stiff	-128 N	-0,187 m
	152 N	0,223 m

From a comparison of the extreme results it can be concluded that the response of the linear models is of a same order as the response of the non-linear model. The stiff linear model gives a small underestimation of the extreme displacements and forces while the less stiff linear model results in a small overestimation of the extreme displacements and forces.